The Core Human Fecal Metabolome

Jacob J. Haffner[1,2], Mitchelle Katemauswa[2,3], Thérèse S. Kagone[4,5], Ekram Hossain[2,3], David Jacobson[1,2], Karina Flores[2,6], Adwaita R. Parab[2,7], Alexandra J. Obregon-Tito[1,2], Raul Y. Tito[1,2], Luis Marin Reyes[8], Luzmila Troncoso-Corzo[9], Emilio Guija-Poma[10,11], Nicolas Meda[4], Hélène Carabin[12,13,14,15], Tanvi P. Honap[1,2], Krithivasan Sankaranarayanan[2,7], Cecil M. Lewis Jr[1,2*], Laura-Isobel McCall[2,3,7*]

[1]Department of Anthropology, University of Oklahoma, Norman, OK, USA. [2]Laboratories of Molecular Anthropology and Microbiome Research (LMAMR), University of Oklahoma, Norman, OK. [3]Department of Chemistry and Biochemistry, University of Oklahoma, Norman, OK, USA. [4]Burkina Faso Ministry of Health, [5]Centre MURAZ Research Institute, Bobo-Dioulasso, Burkina Faso. [6]Department of Biology, University of Oklahoma, Norman, OK, USA. [7]Department of Microbiology and Plant Biology, University of Oklahoma, Norman, OK, USA. [8]Instituto Nacional de Salud, Lima, Peru. [9]Facultad de Medicina, Universidad Nacional Mayor de San Marcos, Lima, Peru. [10]Facultad de Medicina Humana, Universidad de San Martín de Porres, Lima, Peru. [11]Centro de Investigación de Bioquímica y Nutrición, Universidad de San Martín de Porres, Lima, Peru. [12]Department of Biostatistics and Epidemiology, College of Public Health, University of Oklahoma Health Sciences Center, Oklahoma City, OK, USA. [13]Département de Pathologie et Microbiologie, Faculté de médecine vétérinaire, Université de Montréal, Saint-Hyacinthe, QC J2S 2M2, Canada. [14]Département de médecine sociale et préventive, École de santé publique de l'université de Montréal, Montréal, QC H3N 1X9, Canada. [15]Centre de Recherche en Santé Publique (CReSP) de l'université de Montréal et du CIUSS du Centre Sud de Montréal, Montréal, QC H3N 1X9, Canada.

23 *Correspondence and requests for materials can be addressed to C.M.L. (email:

24 cmlewis@ou.edu) and/or L.-I.M. (email: lmccall@ou.edu).

Summary Paragraph

Among the biomolecules at the center of human health and molecular biology is a system of molecules that defines the human phenotype known as the metabolome. Through an untargeted metabolomic analysis of fecal samples from human individuals from Africa and the Americas—the birthplace and the last continental expansion of our species, respectively—we present the characterization of the core human fecal metabolome. The majority of detected metabolite features were ubiquitous across populations, despite any geographic, dietary, or behavioral differences. Such shared metabolite features included hyocholic acid and cholesterol. However, any characterization of the core human fecal metabolome is insufficient without exploring the influence of industrialization. Here, we show chemical differences along an industrialization gradient, where the degree of industrialization correlates with metabolomic changes. We identified differential metabolite features like leucyl-leucine dipeptides and urobilin as major metabolic correlates of these behavioral shifts. Our results indicate that industrialization significantly influences the human fecal metabolome, but diverse human lifestyles and behavior still maintain a core human fecal metabolome. This study represents the first characterization of the core human fecal metabolome through untargeted analyses of populations along an industrialization gradient.

Manuscript

Metabolites fit as the final stage of biology's central dogma: DNA transcribed into RNA translated into proteins which enzymatically interact, form, and shed into small molecules as part of the biochemical pathways of metabolism[1–3]. For this study, we define a metabolite as any small molecule (<1,500 Da) involved in biochemical pathways and the metabolome as the collection of these small molecules within a biological system[3–5]. Using the definition from the Human Metabolome Database, these endogenous metabolites (synthesized by the host) are supplemented by exogenous small molecules (acquired from external sources, such as cosmetics, medication, dietary sources, and pollution)[6]. The human metabolome thus contains both endogenous and exogenous metabolites, representing the nexus of genetic and environmental influences[5,7,8].

Characterizing the fecal metabolome requires an understanding of how it is influenced by different factors, such as industrialization[9,10]. Broadly, industrialization is a series of economic and technological changes relating to the processing and distribution of resources that ultimately cause a shift from agrarian to industrial societies[11,12]. Such changes generally involve an increase in manufactured products compared to agriculture/hunting and other raw products, a greater percentage of workers employed in industrial workplaces over agriculture, and changes in the physical landscape such as increased construction of built environments[13]. Industrialization is often linked with urbanization, which refers to social and demographic shifts increasing population size and density within a settlement[14]. These processes lead to industrialized-urban populations exhibiting denser populations[14], reduced environmental exposures[15,16], an indirect relationship with food sources[17,18], and dietary shifts[18,19] compared to non-industrial rural populations. Moreover, industrialization leads to significant biological changes; industrialization

reduces microbial diversity[16,20–22], increases allergic diseases[23,24] and asthma[25], and heightens susceptibility to illnesses such as inflammatory bowel disease[26,27]. Investigations into industrially-caused metabolomic shifts have identified differences based in amino acids, amines, sphingolipids, and hexoses, among others[19,21,28,29]. Some studies detailed human fecal metabolomes by comparing rural and urban populations and found differences in levels of acylcarnitines, amino acids, and short-chain fatty acids[28–30]. However, such studies employed targeted/semi-targeted metabolomic approaches and/or sampled a single human population[19,21,28–30]. As a result, these studies do not represent ranges of human diversity and behavior, highlighting the need for broader investigations of the human fecal metabolome in terms of geographic range and chemical space.

Here, we performed untargeted liquid chromatography mass spectrometry (LC-MS)-based metabolomics on fecal samples obtained from six human populations from diverse geographic regions (Figure 1a; Table 1; Supplementary Table 1). These populations included male and female children and adults. Our sampled populations were given an industrialization score corresponding with their degree of industrialization from a scale of one (most urban-industrialized) to four (least industrialized; see Materials and Methods for details on score calculation) . Importantly, we included two populations with similar degrees of industrialization but from distinct continents, to control for any geographic confounders - this key aspect has not been considered in prior industrialization-focused metabolomics research. Our populations include: Norman (USA; industrialization score 1); Guayabo (Peru; industrialization score 2); Tambo de Mora (Peru; industrialization score 2); Boulkiemdé (Burkina Faso; industrialization score 3); Tunapuco (Peru; industrialization score 3); and Matses (Peru; industrialization score 4).

Fecal metabolomes of these populations followed an industrialization gradient, where populations exhibited similar metabolomes based on the degree of industrialization. Principal Coordinate Analysis (PCoA) demonstrated significant differences in overall metabolome composition based on industrialization score (Figure 1b-c; Permutational Multivariate Analysis of Variance (PERMANOVA) p=0.001, R^2=0.140; Canberra distance). Moreover, the gradient seen in our data indicates industrialization had a stronger influence on metabolic similarity between populations than geographic origin (Figure 1c; ANOVA industrialization score p=0.046, effect size (eta2)=0.08; ANOVA geographic origin p=0.245, eta2=0.01). This overshadowing of the influence of geography demonstrates the profound influence industrialization has on human molecular biology. Our findings concur with prior studies demonstrating industrialization's role in shaping the human microbiome[31–34], the built environment microbiome[16,35], the built environment metabolome[35], and the plasma metabolome[21]. Additionally, the observation of industrialization outweighing the effects of geographic origin is novel for human fecal metabolomics analyses, but concurs with findings from human fecal microbiome studies[31–34]. To the best of our knowledge, this is the first study to illustrate the industrialization gradient in the human fecal metabolome—the intuitive path for revealing the key chemistry of the distal gut.

To determine the factors driving this clustering of metabolite profiles by industrialization degree, we employed a random forest machine learning algorithm. This random forest analysis analyzed the top 1,000 most abundant metabolites features to identify the 30 most differential metabolite features by degree of industrialization (Table 2; Supplementary Figure 1). Only two of the most abundant differential features could be annotated: leucyl-leucine (mass-to-charge ratio (*m/z*): 245.186; retention time (RT): 3.27 min; Kruskal-Wallis p=8.73e-09) and urobilin (*m/z*: 591.318; RT: 4.52 min; Kruskal-Wallis p=4.45e-07). Leucyl-leucine (leu-leu) abundance

was most associated with non-industrial populations, while urobilin abundance was strongly associated with industrialized populations (Figure 1d-e). Leu-leu is a leucine dipeptide previously recognized as a human metabolite in a study comparing fecal metabolomes of individuals with and without colorectal cancer, where leu-leu showed 99% prevalence across both control and colorectal cancer groups[36]. While leu-leu has not been mentioned in previous industrialization-focused studies of human fecal metabolomes, increased abundance of leucine was noted in fecal metabolomes of urban Nigerian adults as compared to rural adults[28], contrasting with the non-industrial association of leu-leu in our data. The second annotated differential metabolite feature, urobilin, is formed from the metabolic breakdown of hemoglobin[37]. While previous industrialization-focused fecal metabolomics studies did not report this metabolite, urobilin has been identified as a common metabolite in human urine and fecal metabolomes[38,39]. Importantly, urobilin abundance is affected by host diet and behavior[40], with increased abundance seen in populations consuming diets rich in animal fat, proteins, and carbohydrates[41], such as those seen in industrialized populations. Urobilin's association with industrialized human fecal metabolomes highlights the relationship between diet and industrialization, and reinforces the industrialization gradient seen in our results. While only two of the 30 differential metabolite features could be directly annotated, two other features were structurally related to *N*-acetylmuramic acid (MURNAc), as determined by molecular networking[42]. These two features were elevated in semi-industrialized and non-industrialized populations (Figure 1f). MURNAc is a biopolymer component comprising the peptidoglycan layers of bacterial cell walls and a prior study identified reduced abundance of MURNAc in human fecal metabolomes of individuals with lupus[43]. Lupus is an autoimmune disease whose susceptibility is associated with increased environmental exposures that are common to

industrialized populations[44–46]. Since MURNAc is a component of all bacterial cell walls, its association with differential industrialization metabolites also suggests these unannotated metabolite features are bacteria-derived or related. All in all, our results identified several metabolite features that are heavily influenced by industrialization.

Recent research has revealed novel amino acid-conjugated bile acids that are produced by the microbiota[47–49]. Given their enrichment in patients with inflammatory bowel disease[48], which is associated with industrialization processes[26,27], we investigated their distribution across our industrialization gradient. Overall, ten of the 12 total identified amino acid-conjugated bile acids demonstrated a striking increase with industrialization. Such differential amino acid-conjugated bile acids include phenylalanocholic acid (Kruskal-Wallis p=1.9e-6), leucocholic acid (Kruskal-Wallis p=1.69e-7), leucine-conjugated chenodeoxycholic acid (CHDCA) (Kruskal-Wallis p=0.04), tyrosocholic acid (Kruskal-Wallis p=7.71e-3), tyrosine-conjugated deoxycholic acid (Kruskal-Wallis p=1.61e-5), glutamate-conjugated CHDCA (Kruskal-Wallis p=1.69e-7), tryptophan-conjugated CHDCA (Kruskal-Wallis p=4.9e-7), aspartate-conjugated CHDCA (Kruskal-Wallis p=1.13e-5), histidine-conjugated CHDCA (Kruskal-Wallis p=6.41e-3), and histidine-conjugated cholic acid (Kruskal-Wallis p=0.04) (Figure 1g-h, Supplementary Figure 2). However, two amino acid-conjugate bile acids, aspartate-conjugated cholic acid (Kruskal-Wallis p=0.05) and threonine-conjugated CHDCA (Kruskal-Wallis p=0.4), were not enriched in industrialized populations and did not display any statistically significant differences based on industrialization score. The functional role of these amino acid-conjugated bile acids in health is currently unknown, though our results further support a link to industrialization-associated inflammatory diseases.

These differences notwithstanding, our study identified many similarities across populations. A total of 36,324 metabolite features were detected in our samples with 28,288 features being shared across our populations (Figure 2a-b). Our sampled populations are considerably different from each other with strong dietary, behavioral, and geographic differences and, together, represent distinct realms of human experience and diversity. Thus, metabolite features common to these markedly separate populations likely constitute a core human metabolome shared by all humans, even if their abundances vary. To identify these common metabolite features, we filtered our data using three different levels of stringency, limiting metabolite features to those found in at least six individuals from each population, half our samples, or all our samples. The six-sample filtering retained 16,609 total metabolite features across all populations, the half-sample filtering retained 6,205 total metabolite features with 6,008 shared by all populations, and the all-sample filtering retained 1,080 total shared metabolite features. To validate that this high number of shared features was not an artefact of our data processing pipeline, we further filtered our data to only include features shared between two different processing methods: gap-filled and non-gap-filled. Additionally, features annotated to researcher-derived molecules such as DEET were excluded from our list of the core fecal metabolome. These retained common metabolite features included chemical groups like indoles, steroids, lactones, and fatty acyls (Supplementary Table 2; Supplementary Figure 3). Dipeptides included threonylphenylalanine (*m/z* 267.134; RT 0.48 min), valylvaline (*m/z* 217.155; RT 0.45 min), and isoleucylproline (*m/z* 229.155; RT 0.55 min). Shared bile acids include hyocholic acid (*m/z* 158.154; RT 4.78 min; primary bile acid involved with absorbing and transporting diet fats and drugs to the liver[50]) and lithocholic acid (*m/z* 323.273; RT 6.84 min; secondary bile acid commonly found in feces[51] and associated with irritable bowel syndrome[52]). Fatty acid examples

include 3-hydroxydodecanoic acid (*m/z* 199.169; RT 7.10 min; medium chain fatty acid associated with fatty acid metabolic disorders, potentially acquired from the microbial genera *Pseudomonas, Moraxella,* and *Acinetobacter*[53,54]) and palmitoleic acid (*m/z* 237.001; RT 6.42 min; fatty acid commonly found in human adipose tissue and associated with obesity[55]; also acquired in diet from human breast milk[56]). Additional metabolites include cholesterol (*m/z* 369.352; RT 10.5 min; essential sterol found in animals[6]), methionine (*m/z* 105.058; RT 0.33 min; amino acid), and leucine enkephalin (*m/z* 336.192; RT 3.21 min; peptide naturally produced in animal brains, including humans[6,57]). While a number of these shared metabolite features listed above provide key biological functions, some metabolites appear to be derived from dietary sources. An example of a metabolite possibly acquired from food products includes conjugated linoleic acid (*m/z* 263.24; RT 6.68 min; commonly found in meat and dairy products, also recognized for anti-inflammatory capabilities[6,58]).

To explore associations between the core human fecal metabolome and gut microbiome profiles, Spearman's rho correlation coefficients were calculated for the core metabolites and identified microbial operational taxonomic units (OTUs) derived from clustering sequences. Moderate to strong correlations were noted between 604 core human fecal metabolites and gut microbe pairs (Figure 3; Table 3; Supplementary Table 3; Supplementary Files 1-2), though no metabolite-microbe pair reported a correlation coefficient exceeding ±0.6. Most of these metabolites had both positive and negative correlations with different microbes. Many microbes were correlated with multiple metabolites, on average seven. Likewise, on average, each of these 604 metabolites was correlated with 12 microbes, indicating high connectivity between fecal microbiome and metabolome. Extreme examples include methyl-oxindole and bilirubin, which each reported over 40 correlations to microbial OTUs, while Val-Met or Thr-Pro each had only

one correlated microbe. Methyl-oxindole is a tryptophan derivative; metabolism of tryptophan by the gut bacteria has been extensively studied, though methyl-oxindole is less well characterized[59]. Most correlated microbes were categorized as Clostridia (48% of total nodes) or Bacteroidia classes (16% of total nodes) (Figure 3d), which respectively, have reduced and increased abundance in industrialized populations[19,32]. Indeed, urobilin had higher abundance in industrialized than in non-industrialized populations in our analysis, and most of its strong correlations were with Clostridia microbes while most of its negative correlations were with Bacteroidia. Bilirubin, which was enriched in industrialized populations, was negatively correlated with Bacteroidia. This pattern highlights interactions between the core human fecal metabolome and the gut microbiome, especially as they are influenced by processes like industrialization.

Our novel data thus represent a core human fecal metabolome from populations of diverse behaviors and lifestyles, yet we do not presume to have captured the range of diversity of industrial lifestyles or age groups seen in international metabolome initiatives. To broaden our analysis, we co-analyzed our data with a total of 1,286 samples from ten public fecal metabolome datasets[47,49,60–64] (Supplementary Table 4), using the Re-Analysis of Data User Interface (ReDU)[39]. These datasets contained samples from male and female children and adults. Eight of the datasets consisted of samples collected from the United States, one contained samples from Venezuela, and one dataset did not report samples' geographic origin. Furthermore, the datasets included different MS platforms and different metabolite extraction methods, enabling us to assess the commonality of these metabolites across experimental methods. Indeed, every annotated core metabolite (Supplementary Table 2) was detected in this co-analysis, but only 31% were identified in every selected dataset. Such shared annotated

molecules include palmitelaidic acid, urobilin, lithocholic acid, and cholesterol. Furthermore, we also examined the human fecal metabolome database (HFMDB)[65], which contains 6,810 metabolites identified across multiple datasets, for our annotated core metabolite features. 65% of our annotated core metabolite features were present in the HFMDB (Supplementary Table 2); examples of identified metabolites also found in the HFMDB include palmitoleic acid, hypoxanthine, and xanthosine. However, it should be noted that the HFMDB is comprised of data derived from various instrumental, analytical, and processing methods[65]. The absence of some of our core metabolites from the HFMDB can be attributed to these methodological differences.

While we were able to reveal the core human fecal metabolome, only 6.1% of our complete dataset had putative compound-level annotations (level 2 according to the metabolomics standards initiative[66]). Fifteen of these were validated using standards, enabling level 1 confidence[66] (Supplementary Figure 4). 28.8% of the dataset had annotations based only on chemical class (level 3 of the metabolomics standards initiative[66]). This underscores the need for further annotation of human fecal metabolites, especially from human populations traditionally underrepresented in metabolomic databases. Lastly, it is important to note that samples used for this study were collected at different times and subjected to varying preservation treatments and lengths. However, our samples clustered based on industrialization score rather than storage conditions or geographic origin, indicating that any confounding influence from preservation was overshadowed by the effect of industrialization. Full data are freely available on the GNPS[42] and ReDU[39] "living data" infrastructure (see Data Availability statement below) so they can be of use to other researchers and annotations can continue to expand.

Overall, we demonstrate how industrialization profoundly shapes human biology regardless of age, sex, or geographic origin, highlighting the importance of further exploring the biological consequences of industrialization. We also highlight strong commonalities in the fecal metabolome across these distinct populations, representing a core human fecal metabolome of both endogenous and exogenous metabolites. Based on our definition, these chemical components are core to human groups or populations, but not necessarily found in every human individual or LC-MS analysis, given differences in metabolite extraction or instrumental conditions between studies. Further studies focused on untargeted analyses of a spectrum of industrial and non-industrial populations, including past and present humans, can help elucidate the core human fecal metabolome's ubiquity, its relationship with the gut microbiome, and how processes such as industrialization drive human evolution.

Materials and Methods

Project Design

Fecal samples from six human populations were analyzed, representing ranges of industrialization. Populations were assigned industrialization scores to reflect varying degrees of industrialization, based on diet, access to pharmacies and public markets/stores, housing structure, and population density. Score values are: one—highly industrial urban population; two —industrialized rural population; three—a rural community with some industrialization; four—isolated rural community with little to no industrialization. The study populations include: Norman, Oklahoma, USA, a standard Western industrialization population located in the Oklahoma City metropolitan area; Guayabo, Peru, a large rural town influenced by industrialization; Tambo de Mora district, Peru, a large rural district influenced by industrialization; Boulkiemdé province, Burkina Faso, with some industrialization influence; Tunapuco, a traditional rural community located in the Andean Highlands with minimal industrialization influence; and the Matses, an isolated traditional hunter-gatherer community from the Peruvian Amazon (Figure 1; Table 1; Supplementary Table 1). All populations contained both males and females of varying age ranges.

Populations

Fecal samples from Norman, Oklahoma, USA, were analyzed for this project (*n*=18), representing western industrial lifestyles and diets. Norman residents live in the Oklahoma City metropolitan area, exemplifying a highly industrialized environment. Self-reported diets generally consisted of regular dairy consumption plus processed and/or prepackaged foods like

canned vegetables. Due to the strongly industrialized setting and diet, this population received an industrialization score of one.

We also selected fecal samples from the Guayabo (*n*=13) and Tambo de Mora (*n*=17) populations, which practice similar lifestyles. These populations exhibit rural lifestyles and diets but are still strongly influenced by industrialization. Both communities have regular access to public markets and pharmacies and live in densely packed areas. Their diets are generally reliant on foods obtained from these markets, as well as local produce and livestock. While the Guayabo diet commonly consists of maize with some meat and dairy consumption, the Tambo de Mora population relies more on fish, due to their proximity with the Peruvian coastline. Because the Guayabo and Tambo de Mora communities exhibit some characteristics of non-industrial and industrial lifestyles, these populations received an industrialization score of two.

The Boulkiemdé (*n*=11) and Tunapuco (*n*=30**)** communities represent the next degree of industrialization in our sampled populations. Although these populations are from Africa and South America, respectively, they practice similar traditional non-industrial, rural lifestyles and share some features of industrialized populations such as access to public markets. The Boulkiemdé samples were collected from the Boulkiemdé province of Burkina Faso. This Burkinabé community practices an agricultural lifestyle, usually growing their own crops, raising livestock, and with infrequent dairy consumption. Meanwhile, the Tunapuco population have similar traditional agricultural lifestyles, relying on local produce and livestock. Residing in the Peruvian Andes highlands, the Tunapuco people have diets largely consisting of root and stem tubers, bread, and rice. The Tunapuco people occasionally consume animal proteins and dairy products**.** Additionally, Tunapuco residents have access to lowland markets, which offer other dietary sources like fruit. Since both the Boulkiemdé and Tunapuco communities sampled for

this project lived in largely rural yet partly industrial environments, these populations had an industrialization score of three.

Our last sampled population is the Matses (*n*=16). The Matses people practice traditional hunter-gatherer lifestyles, making them unique for this study. Their diet is based heavily on tubers, plantains, fish, and game meat. Dairy and processed foods are very rarely consumed by the Matses community. Due to their location in the Amazonian regions of Peru and unique lifestyles, the Matses are almost completely isolated from external sociocultural and economic influences like industrialization, so they received an industrialization score of four.

Sample Collection

Fecal material was deposited into polypropylene containers and then put in ice. Samples were kept in ice while in the field until arriving at research facilities equipped with freezers. The Norman samples were kept in ice after collection and frozen at the laboratory within 24 hours.

The Peruvian samples were secured similarly to the Norman samples. After collection, samples were stored on ice for four days until arriving at Lima, Peru. Samples were frozen and sent to the laboratory in Norman, Oklahoma.

The Norman, Tunapuco, and Matses samples had previously been aliquoted and underwent 16S rRNA gene sequencing for an earlier study[20], using the MoBio PowerSoil DNA Isolation Kit protocol (full details can be found in the original article[20]). The raw fecal samples were otherwise kept frozen at -80 °C until use for this project.

Boulkiemdé samples were collected similarly to Norman and Peruvian samples. After collection, Boulkiemdé samples were frozen at -20 °C and kept frozen overnight. Samples were thawed the following evening to extract DNA, refrozen at -20 °C, and kept frozen until shipped

to the laboratory in Norman, Oklahoma. Upon arrival, 2 g of fecal material was extracted from each sample for anaerobic culturing. Following this 2 g aliquoting, samples were frozen at -80 °C until use for this project.

Ethics Approval and Informed Consent

Ethical protocols for community engagement and sample collection were developed through collaboration with representatives and authorities from each sampled region and in accordance with institutional regulations. All Peruvian samples were obtained through community engagement with local and national authorities and informed consent with consultation from the Center for Intercultural Health of the Peruvian Institute of Health and Peruvian National Institute of Health ethics committee. This project was reviewed and approved by the research ethics committee of the Instituto Nacional de Salud del Peru (Projects PP-059-11, OEE-036-16).

Human fecal samples were collected with informed consent from resident volunteers in central Burkina Faso under the ethics review committee of Centre MURAZ, a national health research institute in Burkina Faso (IRB ID No. 31/2016/CE-CM). OU IRB deemed this project consistent with US policy 45 CRF 46.101(b) exempt category 4 (OU IRB 6976).

LC-MS/MS Fecal Sample Preparation

The sample preparation protocol used for this project was adapted from a global metabolite extraction protocol with proven success[67]. Samples were thawed and 500 µl of chilled LC-MS grade water (Fisher Scientific) was added to 50 mg of fecal material. Next, a Tissuelyzer homogenized samples at 25 Hz for three minutes. Following homogenization, chilled LC-grade methanol (Fisher Scientific) spiked with 4 µM sulfachloropyridazine as the internal standard (IS)

was added, bringing the total concentration to 50% methanol. The TissueLyzer homogenized samples again at 25 Hz for three minutes, followed by overnight incubation at 4 °C. The next day, samples were centrifuged at 16,000 x g at 4 °C for ten minutes. Aqueous supernatant was then removed and dried using a SpeedVac vacuum concentrator. Dried extracts were frozen at -80 °C until the day of MS analysis. Immediately prior to MS analysis, extracts were resuspended in 150 µl chilled LC-MS methanol:water (1:1) spiked with 1 µg/ml sulfadimethoxine as a second IS. After resuspension, samples were diluted to a 1:10 ratio. Diluted samples were sonicated using a Fisher Scientific Ultrasonic Cleaning Bath at maximum power for ten minutes. Supernatants were spun briefly to remove any particulates, then loaded into a 96-well plate for MS analysis. One well contained only 150 µl of the resuspension solution to serve as a negative control.

LC-MS/MS Analysis

LC was performed on a ThermoFisher Scientific Vanquish Flex Binary LC System with a Kinetex C18 core-shell column (50 x 2.1 mm, 1.7 µM particle size, 100 Å pore size). LC column was kept at 40 °C and the sample compartment was held at 10 °C. The LC System was coupled to a ThermoFisher Scientific Q Exactive Plus Hybrid Quadrupole-Orbitrap Mass Spectrometer for MS/MS analysis. For the LC mobile phase, Solvent A was LC-MS grade water (Fisher Scientific) with 0.1% formic acid and Solvent B was LC-MS grade acetonitrile (Fisher Scientific) with 0.1% formic acid. Elution gradient started at 5% Solvent B for one minute, increased to 100% Solvent B until minute nine, held at 100% Solvent B for two minutes, dropped to 5% Solvent B over 30 seconds, and 5% Solvent B for one minute as re-equilibration. Samples were injected in random order with an injection volume of 5 µl. After elution, electrospray ionization was conducted with spray voltage of 3.8 kV, auxiliary gas flow rate of 10

L/min, auxiliary gas temperature at 350 °C, sheath gas flow rate at 35 L/min, and sweep gas flow at 0 L/min. Capillary temperature was 320 °C and S-lens RF was 50 V.

MS1 scan range was 100-1,500 *m/z*, MS1 resolution was set to 35,000 and MS1 AGC target to 1e6. MS1 data were obtained in positive mode and MS2 data were obtained using data-dependent acquisition. In each cycle, 5 MS/MS scans of the most abundant ion were recorded. Both MS1 and MS2 injection times were set at 100 ms. MS2 resolutions were set to 17,500, MS2 AGC target was set to 5e5, and the inclusion window to 2 *m/z*. MS/MS was conducted at an apex trigger of 2-8 seconds and an exclusion window of 10 seconds. MS/MS collision energy gradually increased from 20-40%.

Authentic standards also underwent LC-MS/MS analysis to validate metabolite annotations. A total of 15 standards were purchased from AA Blocks (hyocholic acid, 13-docosenamide), AvaChem (lenticin), Biosynth (bilirubin, N-acetylmuramic acid, fructosyl-L-lysine), BLD Pharm (N-palmitoylglycine, trans-ferulic acid), ChemScene (leucine enkephalin), LGC Standards (L-saccharopine), Sigma-Aldrich (L-abrine, N-acetyl L-phenylalanine, enoxolone, octadecanamide, lithocholic acid, paraxanthine), and VWR (nicotinamide N-oxide). Each pure standard was diluted to 100 μM, 50 μM, 10 μM, 5 μM, and 1 μM concentrations to maximize standard detection. All standards (and their five dilutions) were analyzed according to the same LC-MS/MS parameters as the original samples. Additionally, fecal extracts with the highest abundance for each standard were re-analyzed as part of the same LC-MS/MS batch to ensure standard peaks were present in samples and to prevent confounding from retention time shifts caused by the gap between initial data acquisition and annotation validation.

Data Analysis and Processing

MSConvert v3.0.19014[68] converted raw data files to mzXML format in preparation for data processing via feature-based molecular networking (FBMN)[69]. MZmine v2.33[70] was used to identify MS features for all samples (Supplementary Table 5). After feature filtering, only features with abundance three times greater than the abundance of blanks were retained in these analyses. Total ion current (TIC) normalization was conducted through R programming language v3.5.3[71] in Jupyter Notebook[72]. FBMN and library spectral database searches were completed using the FBMN workflow on Global Natural Products Social Molecular Networking (GNPS)[42]. FBMN GNPS parameters for MS/MS analysis were as follows: precursor and fragment ion mass tolerance: 0.02 Da, minimum cosine score for networking and library matches: 0.7, minimum number of matched MS2 fragment ions for networking and library matches: 4, network topK: 50, maximum connected component size: 100, maximum shift between precursors: 500 Da, analog search: enabled, maximum analog mass difference: 100 Da, precursor window filtering: enabled, 50 Da peak window filtering: enabled, normalization per file: row sum normalization. Results were analyzed by visually evaluating mirror plot similarity, cosine score, and match likelihood. Molecular networking results were exported to Cytoscape v3.7.1[73] to visualize and analyze networks. Predicted ClassyFire[74] classifications for shared metabolites were derived using the MolNetEnhancer[75] workflow in GNPS. In addition, select annotations were confirmed using authentic standards (Supplementary Figure 4).

MS filtering was performed in MZmine[70]. Three separate filtering workflows were done: 6 minimum peaks in a row (half the number of samples in a single population), 52 minimum peaks in a row (half our total samples), and 105 minimum peaks in a row (all samples). After each filtering step, gap-filling was performed using the previous parameters. For the six-sample filtering, additional processing was done in R[71] to remove any features that were not found in at

least six samples from each population. The resulting files were also analyzed in GNPS as described above.

For 16S rRNA gene sequencing data, we used AdapterRemoval v2[76] to filter out sequences < 90 bp in length. QIIME1[77] was used to perform closed-reference OTU picking using the EzTaxon database[78] as a reference. For OTU picking, the maximum number of database hits per sequence was eight and the maximum number of rejects for a new OTU was 12. After creating biom files, each sample file was rarefied to a depth of 10,000. Generated taxa summaries were limited to genus-level identifications. Only taxa with >0.5% relative frequency were included for correlation analyses.

Correlation and Statistical Analyses

Nonparametric Spearman correlation coefficients were calculated with false discovery rate correction (Supplementary File 1) using metabolite and OTU abundances per sample and per industrialization group. Normalized metabolite feature abundances were summed across each industrialization group using the feature tables derived from R processing via JupyterNotebook. OTU abundances per industrialization group were calculated by determining the relative abundance for each sample and summing the sample abundances according to industrialization score group assignments. Correlation networks with relative MS1 and OTU abundances were visualized using Cytoscape v3.7.1[73]. Weak correlations (correlation coefficient between -0.3 and 0.3) were excluded from subsequent analyses.

Principal coordinate analysis (PCoA) plots were created using Canberra distance metrics from Quantitative Insights Into Microbial Ecology 2 (QIIME2)[79] and visualized using Emperor[80]. PERMANOVA via QIIME2 assessed statistical significance for beta diversity measures.

Kruskal-Wallis p-values were calculated in R[71] through Jupyter Notebook[72]. Boxplots (Figure 1c-h, Supplementary Figures 1-2) were also generated using R[71] in JupyterNotebook[72]. For these boxplots, the center line represents the median, the upper and lower box lines reflect upper and lower quartiles, whiskers reflect the interquartile range multiplied by one-and-a-half, and outliers are dots. R packages ggplot2[81] and rworldmap[82] were used to create Figures 1a, 1c-h,. External visualization tools in GNPS v23[42] were used to create UpSet plots[83]. R package effectsize[84] provided p-values for ANOVA effect size.

To identify metabolite features unique to specific populations or lifestyles, a random forest machine learning algorithm from the R package "randomForest" was used in Jupyter Notebook[85]. The number of trees increased gradually from five until reaching a plateau from out-of-bag error at 200 trees. SIRIUS v4.4.26[86] with ClassyFire[74] classification and CANOPUS[87] compound prediction were used to provide class-level annotations for features identified by random forest.

Data Availability

LC-MS/MS data was uploaded to MassIVE (accession number: MSV000084794). GNPS FBMN jobs are available at https://gnps.ucsd.edu/ProteoSAFe/status.jsp?task=196ab44c10e44c1d898f15e7c046a591 (v21, original analysis) and https://gnps.ucsd.edu/ProteoSAFe/status.jsp?task=505b8b39810c48eb9f9b65fee7c6bc7b (v23, primarily used throughout data analysis). FBMN jobs for filtered data are available at: https://gnps.ucsd.edu/ProteoSAFe/status.jsp?task=db26beb51aff418585e6ad0b92f522b7 (six-sample per population filter, gap-filling), https://gnps.ucsd.edu/ProteoSAFe/status.jsp?task=4693e01a2af740ceb39bfb19720e798d (six-sample per population filter, no gap-filling), https://gnps.ucsd.edu/ProteoSAFe/status.jsp?task=220d1afd0a564ec1818601d3d928d27a (half-sample filter, gap-filling), https://gnps.

ucsd.edu/ProteoSAFe/status.jsp?task=d9686d483e5b496299a02750d6a3ec23 (half-sample filter, no gap-filling), https://gnps.ucsd.edu/ProteoSAFe/status.jsp?task=45150c751a8e42eea51f3ea4936aee95 (all-sample filter, gap-filling), and https://gnps.ucsd.edu/ProteoSAFe/status.jsp?task=45150c751a8e42eea51f3ea4936aee95 (all-sample filter, no gap-filling). ReDU co-analysis is available at https://gnps.ucsd.edu/ProteoSAFe/status.jsp?task=bd266e2a3eba45fa9a1b3819e809a1b6 (co-analysis with fecal data from different MS instruments). Instructions for recreating data analyses in R are available as JupyterNotebook[72] links at: https://github.com/jhaffner09/core_metabolome_2021. 16S data was uploaded to the Qiita database (study ID: 13802).

Public ReDU datasets used for co-analyses are available at: MSV000083559[47] (doi: 10.25345/C5C032; dataset license: CC0 1.0 Universal); MSV000082433[47,62,63] (dataset license: CC0 1.0 Universal); MSV000081351[47] (dataset license: CC0 1.0 Universal); MSV000083756[64] (doi: 10.25345/C53S6N; dataset license: CC0 1.0 Universal); MSV000083300[61] (doi: 10.25345/C56C86; dataset license: CC0 1.0 Universal); MSV000081492[47] (dataset license: CC0 1.0 Universal); MSV000082629[47] (dataset license: CC0 1.0 Universal); MSV000082262 (dataset license: CC0 1.0 Universal); MSV000082221[60] (dataset license: CC0 1.0 Universal); and MSV000082374[49] (dataset license: CC0 1.0 Universal).

References

1. Bino, R. J. *et al.* Potential of metabolomics as a functional genomics tool. *Trends Plant Sci.* **9**, 418–425 (2004).

2. Dettmer, K., Aronov, P. A. & Hammock, B. D. Mass Spectrometry-Based Metabolomics. *Mass Spectrom. Rev.* **26**, 51–78 (2007).

3. Patti, G. J., Yanes, O. & Siuzdak, G. Metabolomics: the apogee of the omic trilogy. *Nat Rev Mol Cell Biol* **13**, 263–269 (2012).

4. Viant, M. R., Kurland, I. J., Jones, M. R. & Dunn, W. B. How close are we to complete annotation of metabolomes? *Curr. Opin. Chem. Biol.* **36**, 64–69 (2017).

5. Johnson, C. H., Ivanisevic, J. & Siuzdak, G. Metabolomics: Beyond biomarkers and towards mechanisms. *Nat. Rev. Mol. Cell Biol.* **17**, 451–459 (2016).

6. Wishart, D. S. *et al.* HMDB 4.0: The human metabolome database for 2018. *Nucleic Acids Res.* **46**, D608–D617 (2017).

7. Wishart, D. S. Emerging applications of metabolomics in drug discovery and precision medicine. *Nat. Rev. Drug Discov.* **15**, 473–484 (2016).

8. Nordström, A., O'Maille, G., Qin, C. & Siuzdak, G. Nonlinear data alignment for UPLC-MS and HPLC-MS based metabolomics: Quantitative analysis of endogenous and exogenous metabolites in human serum. *Anal. Chem.* **78**, 3289–3295 (2006).

9. Lamichhane, S., Sen, P., Dickens, A. M., Orešič, M. & Bertram, H. C. Gut metabolome meets microbiome: A methodological perspective to understand the relationship between host and microbe. *Methods* **149**, 3–12 (2018).

10. Vernocchi, P., Del Chierico, F. & Putignani, L. Gut microbiota profiling: Metabolomics based approach to unravel compounds affecting human health. *Front. Microbiol.* **7**, (2016).

11. Treiman, D. J. Industrialization and Social Stratification. *Sociol. Inq.* **40**, 207–234 (1970).

12. Gollin, D., Jedwab, R. & Vollrath, D. Urbanization with and without industrialization. *J. Econ. Growth* **21**, 35–70 (2016).

13. Simandan, D. Industrialization: Definitions and Measurement. in *International Encyclopedia of Human Geography* (eds. Kitchin, R. & Thrift, N.) 419–425 (2009). doi:https://doi-org.ezproxy.lib.ou.edu/10.1016/B978-008044910-4.00178-4

14. Ritchie, H. & Roser, M. Urbanization. *Publ. online OurWorldInData.org* (2020).

15. Höppe, P. & Martinac, I. Indoor climate and air quality. Review of current and future topics in the field of ISB study group 10. *Int. J. Biometeorol.* **42**, 1–7 (1998).

16. Ruiz-Calderon, J. F. *et al.* Microbiology: Walls talk: Microbial biogeography of homes spanning urbanization. *Sci. Adv.* **2**, (2016).

17. Popkin, B. M. Urbanization, lifestyle changes and the nutrition transition. *World Dev.* **27**, 1905–1916 (1999).

18. Satterthwaite, D., McGranahan, G. & Tacoli, C. Urbanization and its implications for food and farming. *Philos. Trans. R. Soc. B Biol. Sci.* **365**, 2809–2820 (2010).

19. Kisuse, J. *et al.* Urban diets linked to gut microbiome and metabolome alterations in children: A comparative cross-sectional study in Thailand. *Front. Microbiol.* **9**, 1–16 (2018).

518 20. Obregon-Tito, A. J. *et al.* Subsistence strategies in traditional societies distinguish gut
519 microbiomes. *Nat. Commun.* **6**, 1–9 (2015).

520 21. Winglee, K. *et al.* Recent urbanization in China is correlated with a Westernized
521 microbiome encoding increased virulence and antibiotic resistance genes. *Microbiome* **5**,
522 1–13 (2017).

523 22. Stamper, C. E. *et al.* Chapter 14: The Microbiome of the Built Environment and Human
524 Behavior: Implications for Emotional Health and Well-Being in Postmodern Western
525 Societies. in *International Review of Neurobiology* 289–323 (Elsevier Inc., 2016).
526 doi:10.1016/bs.irn.2016.07.006

527 23. Carlsten, C. & Rider, C. F. Traffic-related air pollution and allergic disease: An update in
528 the context of global urbanization. *Curr. Opin. Allergy Clin. Immunol.* **17**, 86–89 (2017).

529 24. Nicolaou, N., Siddique, N. & Custovic, A. Allergic disease in urban and rural populations:
530 Increasing prevalence with increasing urbanization. *Allergy Eur. J. Allergy Clin. Immunol.*
531 **60**, 1357–1360 (2005).

532 25. Ponte, E. V. *et al.* Urbanization is associated with increased asthma morbidity and
533 mortality in Brazil. *Clin. Respir. J.* **12**, 410–417 (2018).

534 26. Abu Freha, N. *et al.* Inflammatory bowel disease among Bedouin Arabs in southern Israel:
535 Urbanization and increasing prevalence rates. *Eur. J. Gastroenterol. Hepatol.* **27**, 230–234
536 (2015).

537 27. Benchimol, E. I. *et al.* Rural and Urban Residence during Early Life is Associated with a
538 Lower Risk of Inflammatory Bowel Disease: A Population-Based Inception and Birth

539 Cohort Study. *Am. J. Gastroenterol.* **112**, 1412–1422 (2017).

540 28. Ayeni, F. A. *et al.* Infant and Adult Gut Microbiome and Metabolome in Rural Bassa and
541 Urban Settlers from Nigeria. *Cell Rep.* **23**, 3056–3067 (2018).

542 29. Turroni, S. *et al.* Fecal metabolome of the Hadza hunter-gatherers: a host-microbiome
543 integrative view. *Sci. Rep.* **6**, 1–9 (2016).

544 30. Zierer, J. *et al.* The fecal metabolome as a functional readout of the gut microbiome. *Nat.*
545 *Genet.* **50**, 790–795 (2018).

546 31. Schnorr, S. L. *et al.* Gut microbiome of the Hadza hunter-gatherers. *Nat. Commun.* **5**, 1–
547 12 (2014).

548 32. Gomez, A. *et al.* Gut Microbiome of Coexisting BaAka Pygmies and Bantu Reflects
549 Gradients of Traditional Subsistence Patterns. *Cell Rep.* **14**, 2142–2153 (2016).

550 33. Mancabelli, L. *et al.* Meta-analysis of the human gut microbiome from urbanized and pre-
551 agricultural populations. *Environ. Microbiol.* **19**, 1379–1390 (2017).

552 34. Yatsunenko, T. *et al.* Human gut microbiome viewed across age and geography. *Nature*
553 **486**, 222–227 (2012).

554 35. McCall, L. I. *et al.* Home chemical and microbial transitions across urbanization. *Nat.*
555 *Microbiol.* (2020). doi:10.1038/s41564-019-0593-4

556 36. Goedert, J. J. *et al.* Fecal metabolomics: Assay performance and association with
557 colorectal cancer. *Carcinogenesis* **35**, 2089–2096 (2014).

558 37. Jones-Lepp, T. L. Chemical markers of human waste contamination: Analysis of urobilin
559 and pharmaceuticals in source waters. *J. Environ. Monit.* **8**, 472–478 (2006).

560 38. Cao, H. *et al.* Fecal metabolome profiling of liver cirrhosis and hepatocellular carcinoma
561 patients by ultra performance liquid chromatography-mass spectrometry. *Anal. Chim. Acta*
562 **691**, 68–75 (2011).

563 39. Jarmusch, A. K. *et al.* Repository-scale Co- and Re-analysis of Tandem Mass
564 Spectrometry Data. *bioRxiv* 750471 (2019). doi:10.1101/750471

565 40. Hill, M. J. The effect of some factors on the faecal concentration of acid steroids, neutral
566 steroids and urobilins. *J. Pathol.* **104**, 239–245 (1971).

567 41. Jain, A., Li, X. H. & Chen, W. N. An untargeted fecal and urine metabolomics analysis of
568 the interplay between the gut microbiome, diet and human metabolism in Indian and
569 Chinese adults. *Sci. Rep.* **9**, 1–13 (2019).

570 42. Wang, M. *et al.* Sharing and community curation of mass spectrometry data with GNPS.
571 *Nat. Biotechnol.* **34**, 828–837 (2016).

572 43. Rojo, D. *et al.* Ranking the impact of human health disorders on gut metabolism: Systemic
573 lupus erythematosus and obesity as study cases. *Sci. Rep.* **5**, 1–9 (2015).

574 44. Kamen, D. L. Environmental influences on systemic lupus erythematosus expression.
575 *Rheum. Dis. Clin. North Am.* **40**, 401–412 (2014).

576 45. Parks, C. G. & De Roos, A. J. Pesticides, chemical and industrial exposures in relation to
577 systemic lupus erythematosus. *Lupus* **23**, 527–536 (2014).

578 46. Leffers, H. C. B., Lange, T., Collins, C., Ulff-Møller, C. J. & Jacobsen, S. The study of
579 interactions between genome and exposome in the development of systemic lupus
580 erythematosus. *Autoimmun. Rev.* **18**, 382–392 (2019).

581 47. Hoffmann, M. A. *et al.* Assigning confidence to structural annotations from mass spectra
582 with COSMIC. *bioRxiv* 2021.03.18.435634 (2021).

583 48. Quinn, R. A. *et al.* Global chemical effects of the microbiome include new bile-acid
584 conjugations. *Nature* **579**, 123–129 (2020).

585 49. Wang, M. *et al.* Mass spectrometry searches using MASST. *Nat. Biotechnol.* **38**, 19–22
586 (2020).

587 50. Chiang, J. Y. L. Bile acid metabolism and signaling in liver disease and therapy. *Liver*
588 *Res.* **1**, 3–9 (2017).

589 51. Ridlon, J. M., Kang, D. J. & Hylemon, P. B. Bile salt biotransformations by human
590 intestinal bacteria. *J. Lipid Res.* **47**, 241–259 (2006).

591 52. Shin, A. *et al.* Bowel functions, fecal unconjugated primary and secondary bile acids, and
592 colonic transit in patients with irritable bowel syndrome. *Clin. Gastroenterol. Hepatol.* **11**,
593 1270-1275.e1 (2013).

594 53. Chickos, J. S. *et al.* Analysis of 3-hydroxydodecanedioic acid for studies of fatty acid
595 metabolic disorders: Preparation of stable isotope standards. *J. Clin. Lab. Anal.* **16**, 115–
596 120 (2002).

597 54. Ktsoyan, Z. A. *et al.* Profiles of microbial fatty acids in the human metabolome are
598 disease-specific. *Front. Microbiol.* **1**, 1–9 (2011).

599 55. Gong, J. *et al.* Adipose tissue palmitoleic acid and obesity in humans: Does it behave as a
600 lipokine? *Am. J. Clin. Nutr.* **93**, 186–191 (2011).

601 56. Ogunleye, A. *et al.* Fatty Acid Composition of Breast Milk from Nigerian and Japanese

602 Women. *J. Nutr. Sci. Vitaminol. (Tokyo).* **37**, 435–442 (1991).

603 57. Ozalp, A., Barroso, B., Meijer, J. & van den Beld, C. Determination of methionine-
604 enkephalin and leucine-enkephalin by LC-MS in human plasma: Study of pre-analytical
605 stability. *Anal. Biochem.* **559**, 24–29 (2018).

606 58. Lee, Y., Thompson, J. T. & Vanden Heuvel, J. P. 9E,11E-Conjugated Linoleic Acid
607 Increases Expression of the Endogenous Antiinflammatory Factor, Interleukin-1 Receptor
608 Antagonist, in RAW 264.7 Cells. *J. Nutr.* **139**, 1861–1866 (2009).

609 59. Dong, F. *et al.* Intestinal microbiota-derived tryptophan metabolites are predictive of Ah
610 receptor activity. *Gut Microbes* **12**, 1–24 (2020).

611 60. Fang, X. *et al.* Gastrointestinal Surgery for Inflammatory Bowel Disease Persistently
612 Lowers Microbiome and Metabolome Diversity. *Inflamm. Bowel Dis.* **27**, 603–616 (2021).

613 61. Mu, A. *et al.* Assessment of the microbiome during bacteriophage therapy in combination
614 with systemic antibiotics to treat a case of staphylococcal device infection. *Microbiome* **9**,
615 1–8 (2021).

616 62. Petras, D. *et al.* Non-Targeted Metabolomics Enables the Prioritization and Tracking of
617 Anthropogenic Pollutants in Coastal Seawater. *ChemArxiv* **1**, 1–25 (2019).

618 63. Petras, D. *et al.* Non-targeted tandem mass spectrometry enables the visualization of
619 organic matter chemotype shifts in coastal seawater. *Chemosphere* **271**, 129450 (2021).

620 64. Tripathi, A. *et al.* Chemically informed analyses of metabolomics mass spectrometry data
621 with Qemistree. *Nat. Chem. Biol.* **17**, 146–151 (2021).

622 65. Karu, N. *et al.* A review on human fecal metabolomics: Methods, applications and the

human fecal metabolome database. *Anal. Chim. Acta* **1030**, 1–24 (2018).

66. Sumner, L. W. *et al.* Proposed minimum reporting standards for chemical analysis: Chemical Analysis Working Group (CAWG) Metabolomics Standards Initiative (MSI). *Metabolomics* **3**, 211–221 (2007).

67. Want, E. J. *et al.* Global metabolic profiling of animal and human tissues via UPLC-MS. *Nat. Protoc.* **8**, 17–32 (2013).

68. Chambers, M. C. *et al.* A cross-platform toolkit for mass spectrometry and proteomics. *Nat. Biotechnol.* **30**, 918–920 (2012).

69. Nothias, L. F. *et al.* Feature-based Molecular Networking in the GNPS Analysis Environment. *bioRXiv* (2019).

70. Pluskal, T., Castillo, S., Villar-Briones, A. & Orešič, M. MZmine 2: Modular framework for processing, visualizing, and analyzing mass spectrometry-based molecular profile data. *BMC Bioinformatics* **11**, (2010).

71. Bunn, A. & Korpela, M. R: A Language for Data Analysis and Graphics. *Ind. Commer. Train.* **0**, 1–16 (2018).

72. Kluyver, T. *et al.* Jupyter Notebooks—a publishing format for reproducible computational workflows. *Position. Power Acad. Publ. Play. Agents Agendas* 87–90 (2016). doi:10.3233/978-1-61499-649-1-87

73. Shannon, P. *et al.* Cytoscape: A Software Environment for Integrated Models. *Genome Res.* **13**, 2498–2504 (2003).

74. Djoumbou Feunang, Y. *et al.* ClassyFire: automated chemical classification with a

644 comprehensive, computable taxonomy. *J. Cheminform.* **8**, 1–20 (2016).

645 75. Ernst, M. *et al.* MolNetEnhancer: Enhanced Molecular Networks by Integrating
646 Metabolome Mining and Annotation Tools. *Metabolites* **9**, 144 (2019).

647 76. Schubert, M., Lindgreen, S. & Orlando, L. AdapterRemoval v2: rapid adapter trimming,
648 identification, and read merging. *BMC Res. Notes* **9**, 88 (2016).

649 77. Caporaso, J. G. *et al.* QIIME allows analysis of high-throughput community sequencing
650 data. *Nat. Methods* **7**, 335–336 (2010).

651 78. Chun, J. *et al.* EzTaxon: A web-based tool for the identification of prokaryotes based on
652 16S ribosomal RNA gene sequences. *Int. J. Syst. Evol. Microbiol.* **57**, 2259–2261 (2007).

653 79. Bolyen, E. *et al.* Reproducible, interactive, scalable and extensible microbiome data
654 science using QIIME 2. *Nat. Biotechnol.* **37**, 852–857 (2019).

655 80. Vázquez-Baeza, Y., Pirrung, M., Gonzalez, A. & Knight, R. EMPeror: A tool for
656 visualizing high-throughput microbial community data. *Gigascience* **2**, 2–5 (2013).

657 81. Wickham, H. *Ggplot2: Elegant Graphics for Data Analysis*. (Springer US, 2016).

658 82. South, A. rworldmap: A new R package for mapping global data. *R J.* **3**, 35–43 (2011).

659 83. Lex, A., Gehlenborg, N., Strobelt, H., Vuillemot, R. & Pfister, H. UpSet: Visualization of
660 intersecting sets. *IEEE Trans. Vis. Comput. Graph.* **20**, 1983–1992 (2014).

661 84. Ben-Shachar, M., Makowski, D. & Lüdecke, D. Compute and interpret indices of effect
662 size. *CRAN* (2020).

663 85. Liaw, A. & Wiener, M. Classification and Regression by RandomForest. *R News* **3**, 18–22

(2002).

86. Dührkop, K. *et al.* SIRIUS 4: a rapid tool for turning tandem mass spectra into metabolite structure information. *Nat. Methods* **16**, 299–302 (2019).

87. Dührkop, K. *et al.* Classes for the masses: Systematic classification of unknowns using fragmentation spectra. *bioRxiv* 2020.04.17.046672 (2020). doi:10.1101/2020.04.17.046672

88. Kim, S. *et al.* PubChem in 2021: New data content and improved web interfaces. *Nucleic Acids Res.* **49**, D1388–D1395 (2021).

673 **Figures**

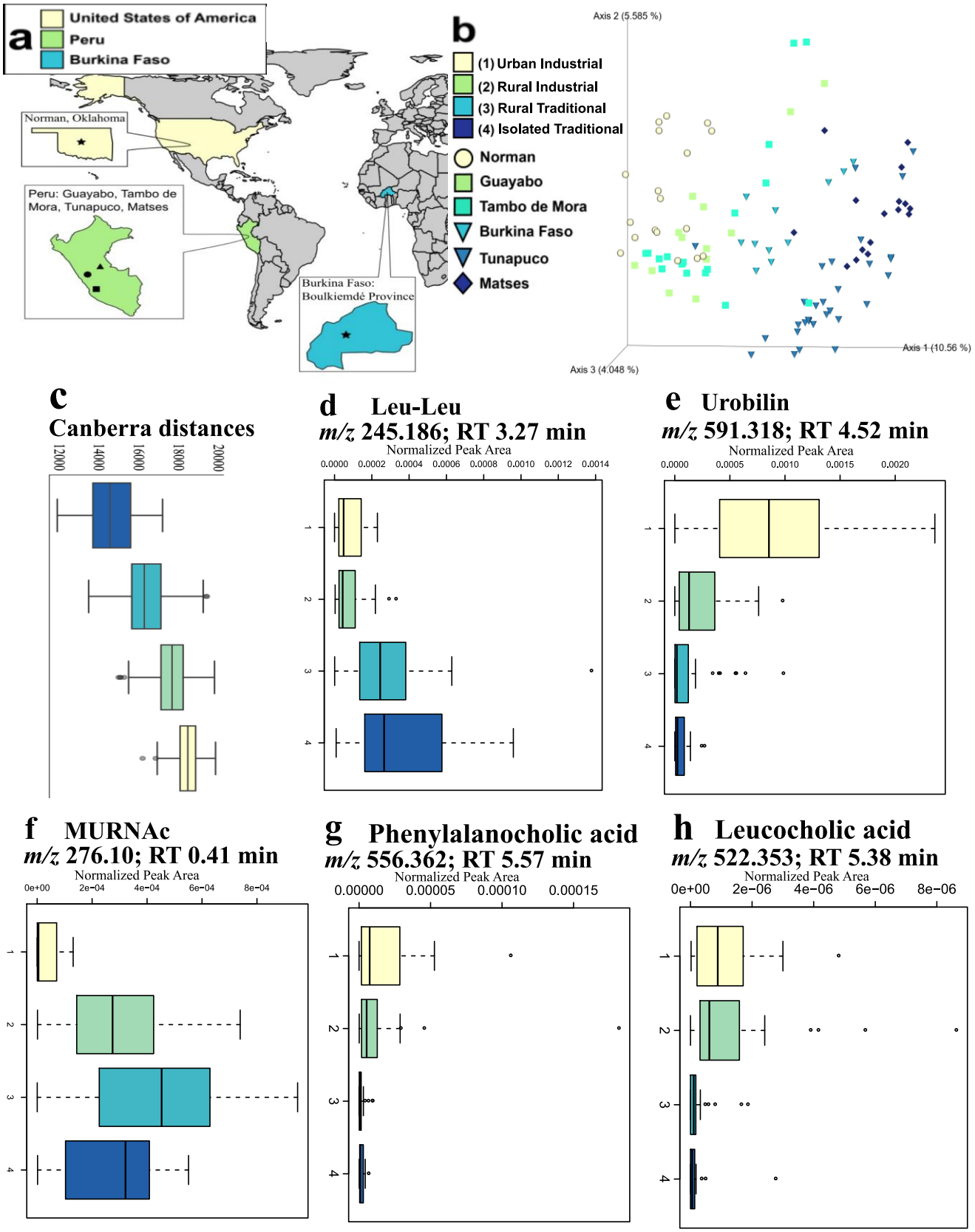

Figure 1. Fecal metabolomic profiles follow an industrialization gradient.

a, Sampling sites. Tan star: Norman; Green circle: Guayabo; Green square: Tambo de Mora; green triangle: Tunapuco; Blue star: Boulkiemdé.Matses left unmarked due to privacy concerns. **b** Principal coordinate analysis (Canberra distance metric) depicts industrialization gradient. Colored by industrialization score and shape-coded by population. **c**, Calculated Canberra distances follow an industrialization gradient. Colored by industrialization score. Color key from **b** applies to **c-i. d-f**, Normalized abundances of features identified by random forest differing by industrialization score: **d**, Leucyl-leucine (leu-leu), associated with non-industrialized populations. *m/z* 245.186; RT 3.27 min. **e**, Urobilin, associated with industrialized populations. *m/z* 591.318; RT 4.16 min. **f**, Feature structurally similar to *N*-acetylmuramic acid (MURNAc) associated with semi-industrialized and non-industrialized populations, *m/z* 276.108; RT 0.41 min. **g-h**, Normalized abundances of novel amino acid-conjugated bile acids depict an industrialization gradient: **g**, Phenylalanocholic acid. *m/z* 556.36; RT 5.57 min. **h**, Leucocholic acid. *m/z* 522.353; RT 5.38 min.

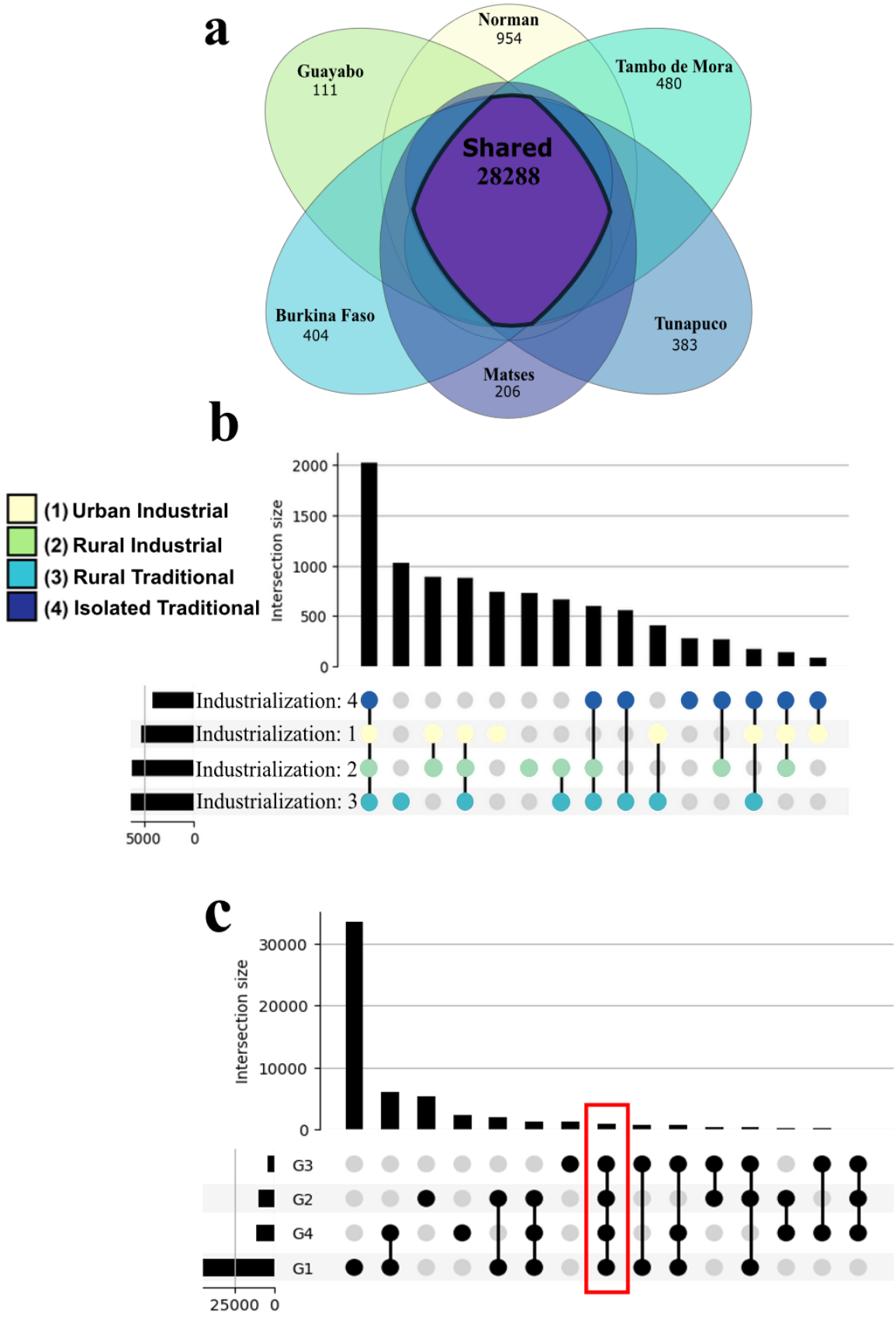

720

Figure 2. The core human metabolome.
a, Metabolic feature overlap across study populations. **b**, UpSet plot of industrialization score sets indicate strong similarity of metabolomic profiles. **c**, UpSet plot of ReDU co-analysis datasets sorted by MS instrument. G1 is ThermoFisher Scientific Q Exactive (*n*=696); G2 is Bruker Impact (*n*=447); G3 is Bruker maXis (*n*=143); G4 is the dataset from this study (*n*=105). The co-analysis illustrates overlap across the datasets, despite instrumental differences. Colored box highlights intersection of all datasets (855 total metabolite feature).

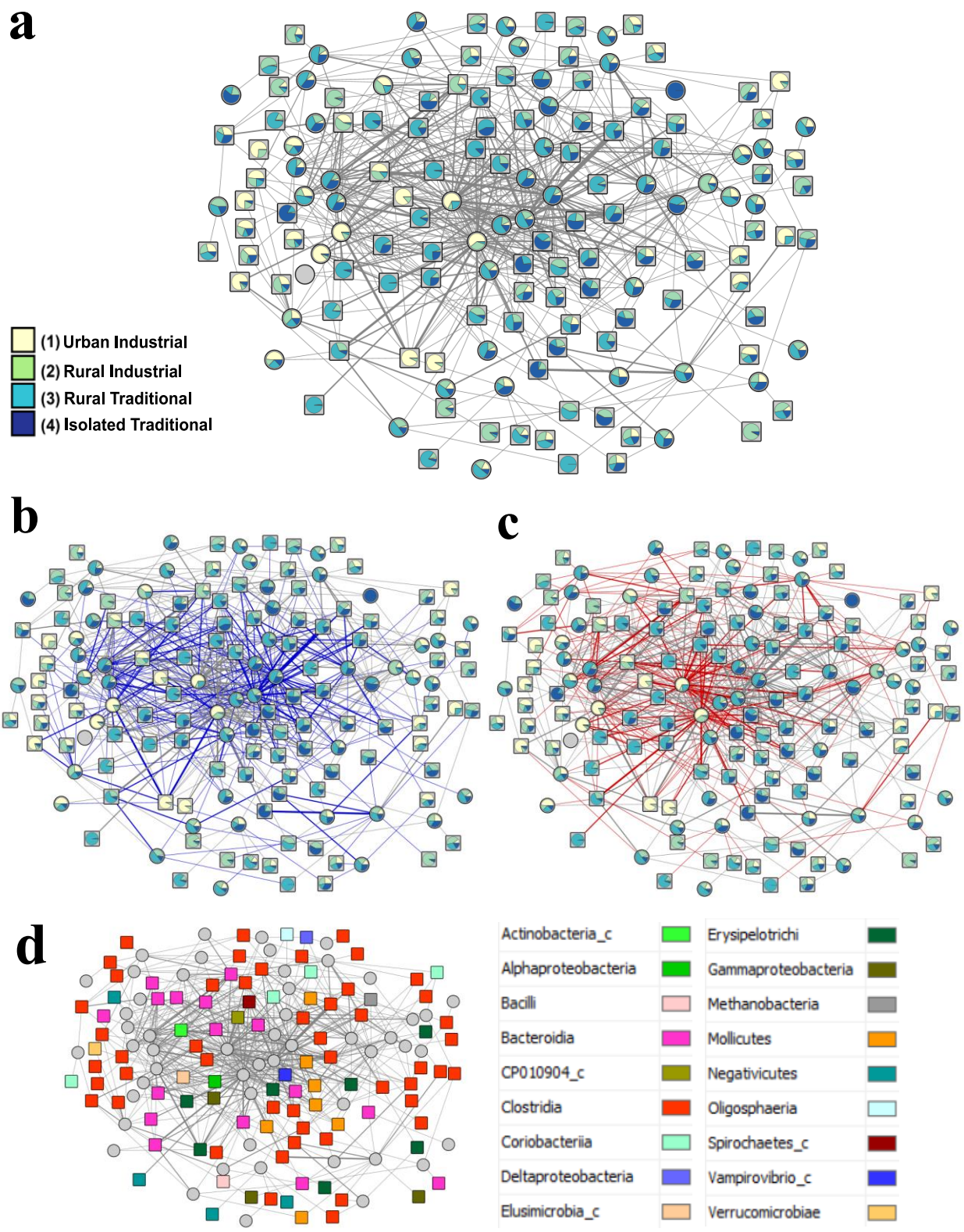

Figure 3. Correlation network of metabolite-microbe associations across an urbanization gradient.

735 **a,** Correlation network. **a-d**, Metabolites are circles and microbial OTUs are squares. **a-c**, Thin
736 edges represent weak correlations (±0.3 - ±0.399), medium edges are moderate correlations (±0.4
737 - ±0.499), and thick edges are moderately strong correlations (>±0.5). Pie charts represent node
738 abundance across industrialization groups. Color key from **a** applies to **b-c**. **b,** Positive
739 correlations are blue. **c,** Negative correlations are red. **d**, Microbes are color-coded by microbial
740 class. Clostridia is the predominant microbial class represented in the correlation network,
741 followed by Bacteroidia and Mollicutes.
742
743
744
745
746
747
748

749 **Tables**

750

751 **Table 1. Sampled population metadata.**

					Age distribution			Sex distribution	
Population	Abbreviation	Geographic Origin	Industrialization Score	Sample size (n)	1-17 years	18-44 years	45+ years	Female	Male
Total			1-4	105	39	48	17	50	34
Norman	NO	Norman, Oklahoma, United States	1	18	0	18	0	7	11
Guayabo	GU	Guayabo, Peru, South America	2	13	5	7	5	11	0
Tambo de Mora	TM	Tambo de Mora District, Peru, South America	2	17	8	5	3	8	1
Boulkiemdé	BF	Boulkiemdé Province, Burkina Faso, Africa	3	11	0	6	5	6	5
Tunapuco	HCO	Andean Highlands, Peru, South America	3	30	15	9	2	17	9
Matses	SM	Peruvian Amazon, South America	4	16	11	3	2	8	8

752 **Table 2. Top 30 most differential metabolite features as determined by random forest classifier.**
753

Feature	*m/z*	RT (min)	p-value (Kruskal-Wallis)	Annotation	Details	Predicted Classyfire[74]/CANOPUS[87] Chemical Class with posterior probability	Mass difference to reference	Adduct	Cosine Score
1	145.13	0.321	1.05E-09	-	-	-	-	-	-
2	145.13	0.322	1.62E-09	-	Part of same sub-network as Feature 1	-	-	-	-
3	159.15	0.359	3.65E-09	-	-	-	-	-	-
4	235.17	0.251	2.28E-07	-	-	Primary alcohol (71.332%)	-	-	-
5	245.19	3.274	8.73E-09	Spectral Match to Leu-Leu	In sub-network with other Leu-Leu spectral matches	Amino acid derivative (87.591%)	0	M+H	0.89
6	276.11	0.411	8.68E-09	-	Part of sub-network with matches to N-Acetylmuramic acid	Organic phosphoric acid and derivatives (59.786%)	-	-	-
7	276.11	0.423	1.43E-06	-	Connected to 2 sub-networks, including the sub-network with Feature 6. Also part of network with matches to Glycan Lacto-N-biose and N-Acetylmuramic acid	Organic phosphoric acid and derivatives (59.786%)	-	-	-
8	286.18	1.41	4.75E-05	-	-	Secondary carboxylic acid amide (54.113%)	-	-	-
9	286.18	1.677	7.10E-06	-	Part of same sub-network as Feature 8	Secondary carboxylic acid amide (54.113%)	-	-	-
10	305.19	3.744	2.66E-06	-	-	Carbamate esters (70.111%)	-	-	-
11	332.07	0.36	6.36E-08	-	-	Aryl chloride (83.961%)	-	-	-

12	363.21	1.018	1.76E-08	-	-	Monosaccharide (59.675%)	-	-	-
13	363.21	0.874	1.78E-06	-	Part of same sub-network as Feature 12	Monosaccharide (59.675%)	-	-	-
14	365.19	0.514	7.39E-09	-	-	Monosaccharide (56.026%)	-	-	-
15	379.3	4.804	4.91E-12	-	-	Lipid and lipid-like molecule (53.344%)	-	-	-
16	379.3	4.823	1.17E-10	-	Part of same sub-network as Feature 15	Lipid and lipid-like molecule (53.344%)	-	-	-
17	379.3	4.804	4.25E-12	-	Part of same sub-network as Features 15 & 16	Lipid and lipid-like molecule (53.344%)	-	-	-
18	379.3	4.811	1.56E-10	-	Part of same sub-network as Features 15, 16, 17	Lipid and lipid-like molecule (53.344%)	-	-	-
19	398.34	4.761	1.28E-07	-	-	Fatty acid ester (60.662%)	-	-	-
20	398.34	4.829	9.19E-08	-	-	Fatty acid ester (60.662%)	-	-	-
21	398.34	4.842	1.15E-07	-	-	Fatty acid ester (60.662%)	-	-	-
22	398.34	4.807	1.65E-07	-	-	Fatty acid ester (60.662%)	-	-	-
23	400.36	4.832	8.29E-07	-	-	-	-	-	-
24	414.34	4.493	3.73E-09	-	-	-	-	-	-
25	414.34	4.428	1.18E-09	-	-	Fatty acid ester (63.169%)	-	-	-
26	414.34	4.379	1.07E-10	-	-	Fatty acid ester (63.169%)	-	-	-
27	414.34	4.428	9.24E-11	-	-	Fatty acid ester (63.169%)	-	-	-
28	591.32	4.516	4.45E-07	Spectral match to Urobilin	Part of sub-network with matches to Bilirubin	Fatty acid ester (77.006%)	0	M+H	0.79
29	593.33	4.979	3.03E-09	-	-	6-alkylaminopurine (51.054%)	-	-	-
30	597.37	5.313	3.27E-06	-	-	Depsipeptide (68.585%)	-	-	-

754

Table 3. Metabolite-Microbe correlations.

Only metabolite-microbe pairs greater than ±0.3 were included. Major microbial class was determined by calculating the percentage of microbial nodes connected to the respective metabolite node, focused on classes with greater than 10% for each respective metabolite.

m/z	RT (min)	Metabolite Name	Number of Edges	Major Taxa Class (%)
137.046	0.38	Hypoxanthine	25	Bacteroidia (24%); Clostridia (24%); Mollicutes (20%)
139.05	0.31	Nicotinamide N-oxide	1	Clostridia (100%)
148.076	3.22	3-methyl-2-oxindole	41	Clostridia (43.9%)
158.154	4.78	Hyocholic acid	12	Clostridia (50%)
177.055	4.13	3-Hydroxy-4-methoxycinnamic acid	11	Clostridia (72.7%)
177.164	5.91	2-Butanone, 4-(2,6,6-trimethyl-2-cyclohexen-1-yl)-	3	Clostridia (66.6%); Bacteroidia (33.3%)
181.072	0.81	Paraxanthine	39	Clostridia (25.6%); Bacteroidia (23.1%)
195.065	3.01	trans-Ferulic acid	9	Clostridia (66.7%)
197.117	3.10	Loliolide	15	Clostridia (53.3%); Bacteroidia (26.7%)
199.169	5.35	3-Hydroxydodecanoic acid	7	Clostridia (28.6%)

204.087	3.53	N-Acetyl-D-mannosamine	8	Bacteroidia (37.5%); Clostridia (37.5%)
208.097	2.84	L-Phenylalanine, N-acetyl-	24	Clostridia (62.5%)
217.122	0.462	Thr-Pro	1	Bacteroidia (100%)
217.155	0.45	Val-Val	10	Bacteroidia (40%); Clostridia (20%)
220.118	0.56	Pantothenic acid	4	Bacteroidia (75%); Clostridia (25%)
227.201	5.94	Myristoleic acid	9	Clostridia (44.4%); Mollicutes (33.3%)
229.155	0.78	Ile-Pro	4	Clostridia (50%); Bacteroidia (25%); Coriobacteriia (25%)
231.171	2.82	Val-Ile	37	Clostridia (35.1%); Bacteroidia (18.9%)
237.221	6.49	cis-9-Hexadecenoic acid	7	Clostridia (42.9%); Negativicutes (28.6%)
239.102	0.44	Gly-Tyr	5	Erysipelotrichi (40%)
245.098	2.39	Biotin	3	Bacteroidia (33.3%); Clostridia (33.3%); Deltaproteobacteria (33.3%)
245.186	2.40	Leu-Leu	23	Bacteroidia (43.5%); Clostridia (21.7%)
247.145	1.22	Lenticin	14	Bacteroidia (50%)
249.126	0.56	Val-Met	1	Clostridia (100%)

263.237	6.68	Conjugated linoleic acid (9E,11E)	14	Clostridia (78.6%)
263.237	7.52	Conjugated linoleic acid (10E,12Z)	1	Clostridia (100%)
267.134	0.48	Thr-Phe	2	Clostridia (50%); Deltaproteobacteria (50%)
272.171	0.32	Pro-Arg	12	Clostridia (83.3%)
275.201	4.42	9-OxoOTrE	4	Clostridia (75%)
279.171	3.47	Leu-Phe	22	Clostridia (36.4%)
282.279	6.09	N-Tetracosenoyl-4-sphingenine	7	Clostridia (71.4%)
285.083	0.40	Xanthosine	23	Bacteroidia (26%); Clostridia (26%)
288.203	0.37	Arg-Ile	25	Bacteroidia (32%); Clostridia (28%)
291.268	5.54	cis-11,14-Eicosadienoic acid	3	Clostridia (66%)
294.119	0.38	N-Acetylmuramic acid	5	Bacteroidia (60%)
297.126	3.14	Phe-Met	3	Actinobacteria (33.3%); Clostridia (33.3%); Coriobacteriia (33.3%)
302.205	3.05	Ile-Gly-Ile	1	Clostridia (100%)

304.166	3.02	Val-Trp	23	Clostridia (52.2%); Mollicutes (17.4%)
309.164	0.313	Fructoselysine	3	Bacteroidia (66.7%); Clostridia (33.3%)
318.167	2.27	Ile-Trp	4	Bacteroidia (50%); Clostridia (50%)
323.273	6.84	Lithocholic acid	14	Clostridia (57.1%)
336.192	3.22	Leucine Enkephalin	4	Bacteroidia (50%); Clostridia (50%)
338.342	9.19	13-Docosenamide, (Z)-	4	Bacteroidia (50%); Clostridia (25%); Spirochaetes (25%)
359.266	0.60	Ile-Val-Lys	2	Clostridia (100%)
369.352	10.51	Cholesterol	2	Bacteroidia (50%); Erysipelotrichi (50%)
405.264	4.82	(R)-4-((3R,5S,8R,9S,10S,13R,14S,17R)-3-hydroxy-10,13-dimethyl-7,12-dioxohexadecahydro-1H-cyclopenta[a]phenanthren-17-yl)pentanoic acid	2	Bacteroidia (50%); Erysipelotrichi (50%)
439.359	7.62	Oleanolic acid	12	Bacteroidia (33.3%)
471.347	6.92	Enoxolone	23	Clostridia (39.1%)

585.272	8.90	Bilirubin	41	Bacteroidia (29.3%); Clostridia (26.8%); Mollicutes (12.2%)
591.318	4.08	Urobilin	14	Bacteroidia (42.9%); Clostridia (28.6%)
595.349	4.05	Stercobilin	5	Clostridia (80%)
839.565	5.12	Cholic acid	15	Clostridia (40%); Mollicutes (26.7%)

758

Supplementary Tables and Figures

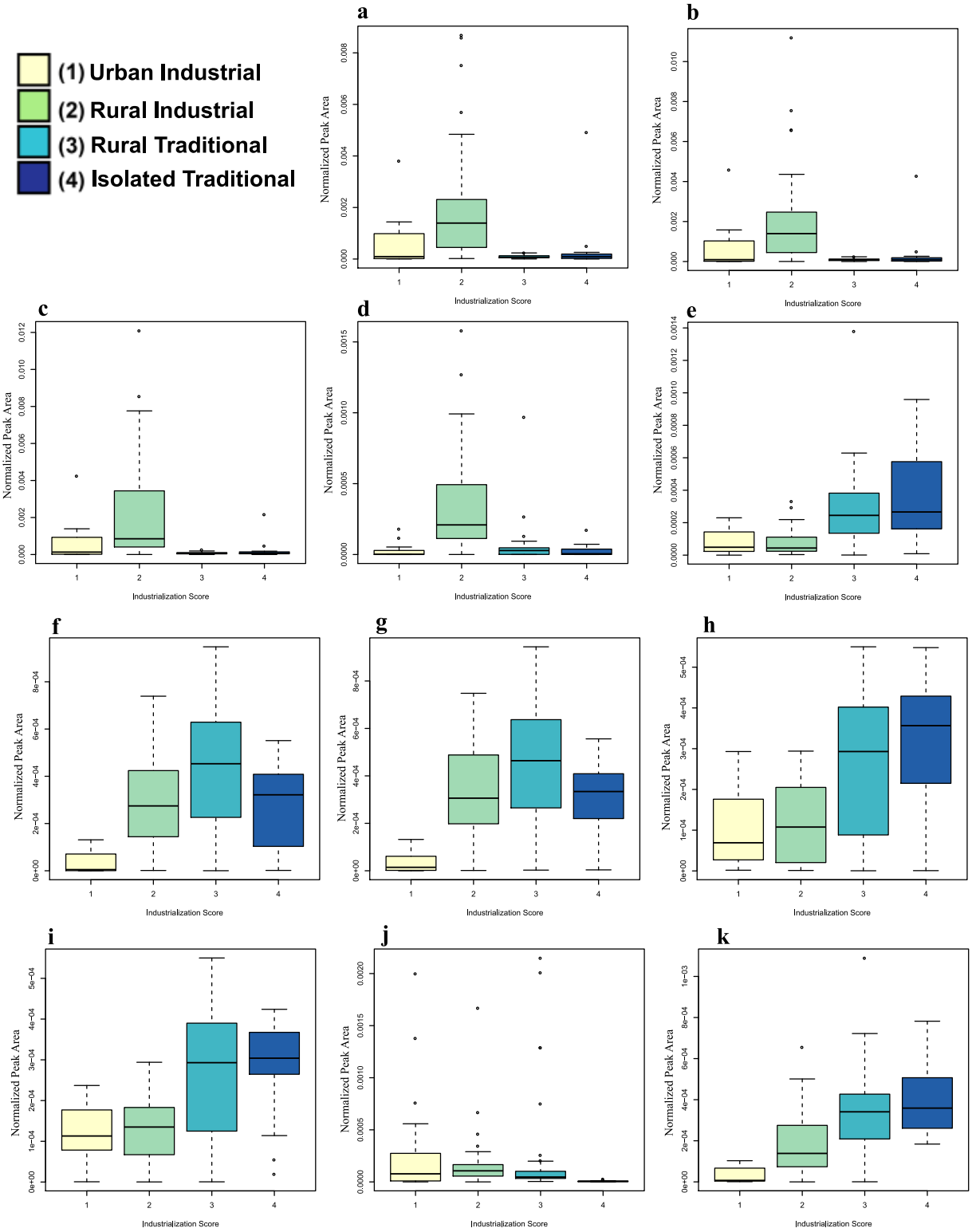

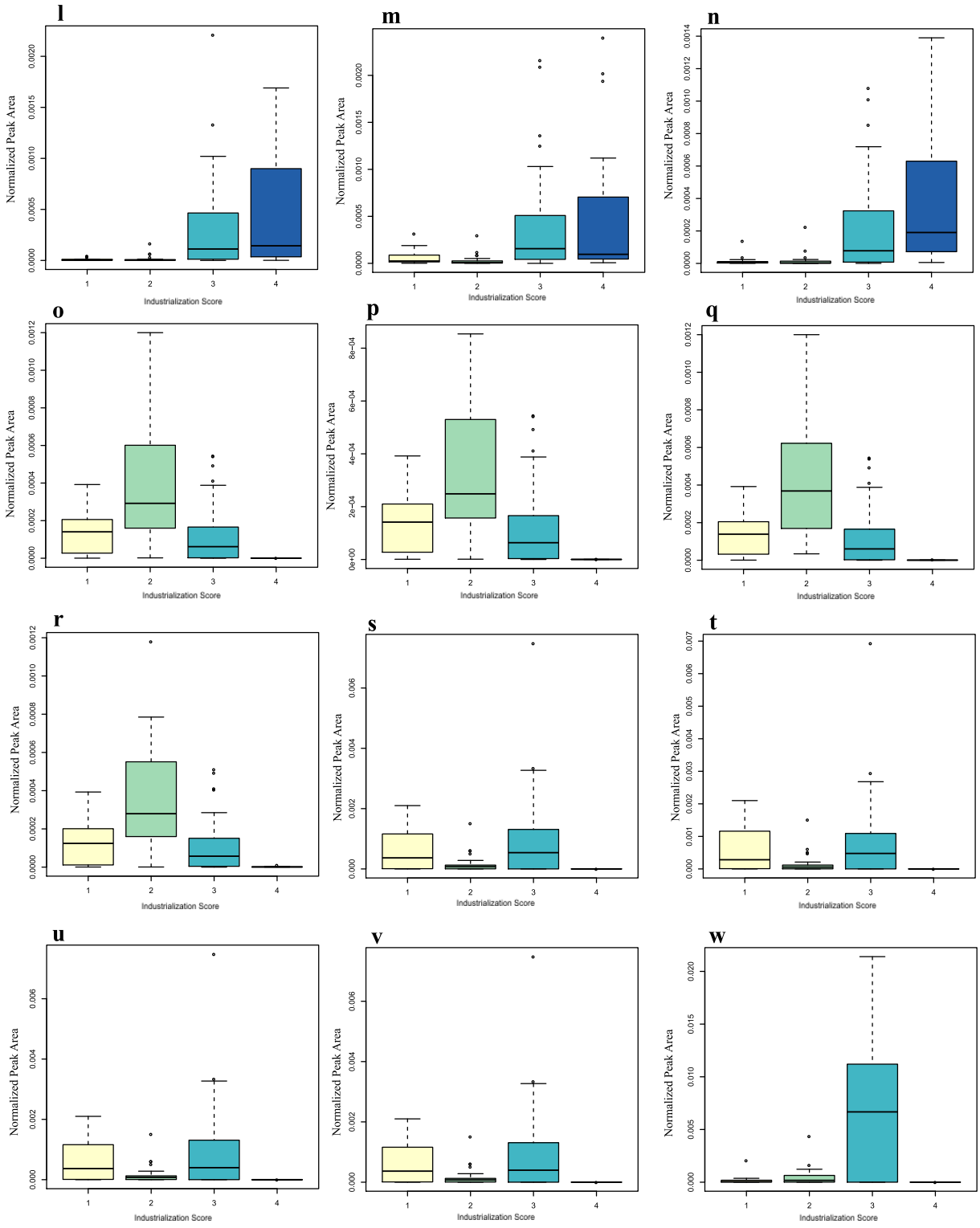

760
761

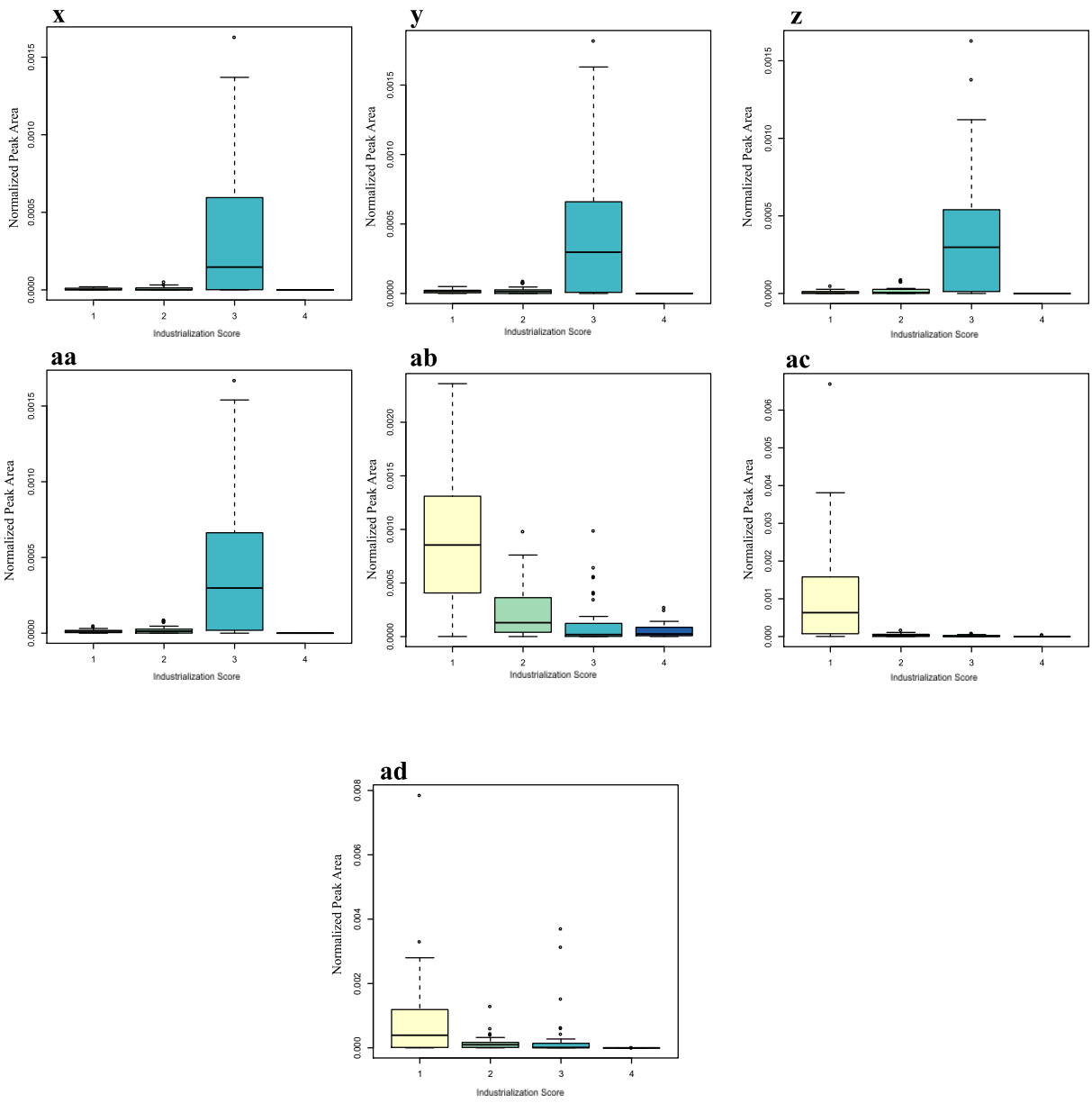

762

Supplementary Figure 1. Abundances of top 30 differential metabolite features based on industrialization score identified by RandomForest.

Color key applies for figures **a-ad**. **a,** *m/z* 145.134, RT 0.32 min; **b,** *m/z* 145.134, RT 0.32 min; **c,** *m/z* 145.1340, RT 0.36 min; **d**, *m/z* 235.166, RT 0.25 min; **e,** *m/z* 246.186, RT 3.27 min; **f,** 276.108, RT 4.41 min; **g,** *m/z* 276.108, 0.42; **h,** *m/z* 286.176, RT 1.41 min; **i,** *m/z* 286.176, RT 1.677 min; **j,** *m/z* 305.186, RT 3.74 min; **k,** *m/z* 332.074, RT 0.36 min; **l,** *m/z* 363.211, RT 1.02; **m,** *m/z* 363.213, RT 0.87 min; **n,** *m/z* 365.192, RT 0.51 min; **o,** *m/z* 379.295, RT 4.8 min; **p,** *m/z* 379.296, RT 4.82 min; **q,** *m/z* 379.296, RT 4.8 min; **r,** *m/z* 379.297, RT 4.81 min; **s,** *m/z* 398.342, RT 4.76 min; **t,** *m/z* 398.342, RT 4.82 min; **u,** *m/z* 398.342, RT 4.84 min; **v,** *m/z* 398.345, RT 4.81 min; **w,** *m/z* 400.358, RT 4.83 min; **x,** *m/z* 414.335, RT 4.49 min; **y,** *m/z* 414.337, RT 4.43 min; **z,** *m/z* 414.337, RT 4.38 min; **aa,** *m/z* 414.337, RT 4.43 min; **ab,** 591.318, RT 4.52; **ac,** *m/z* 593.333, RT 4.98 min; **ad,** *m/z* 597.37, RT 5.31 min.

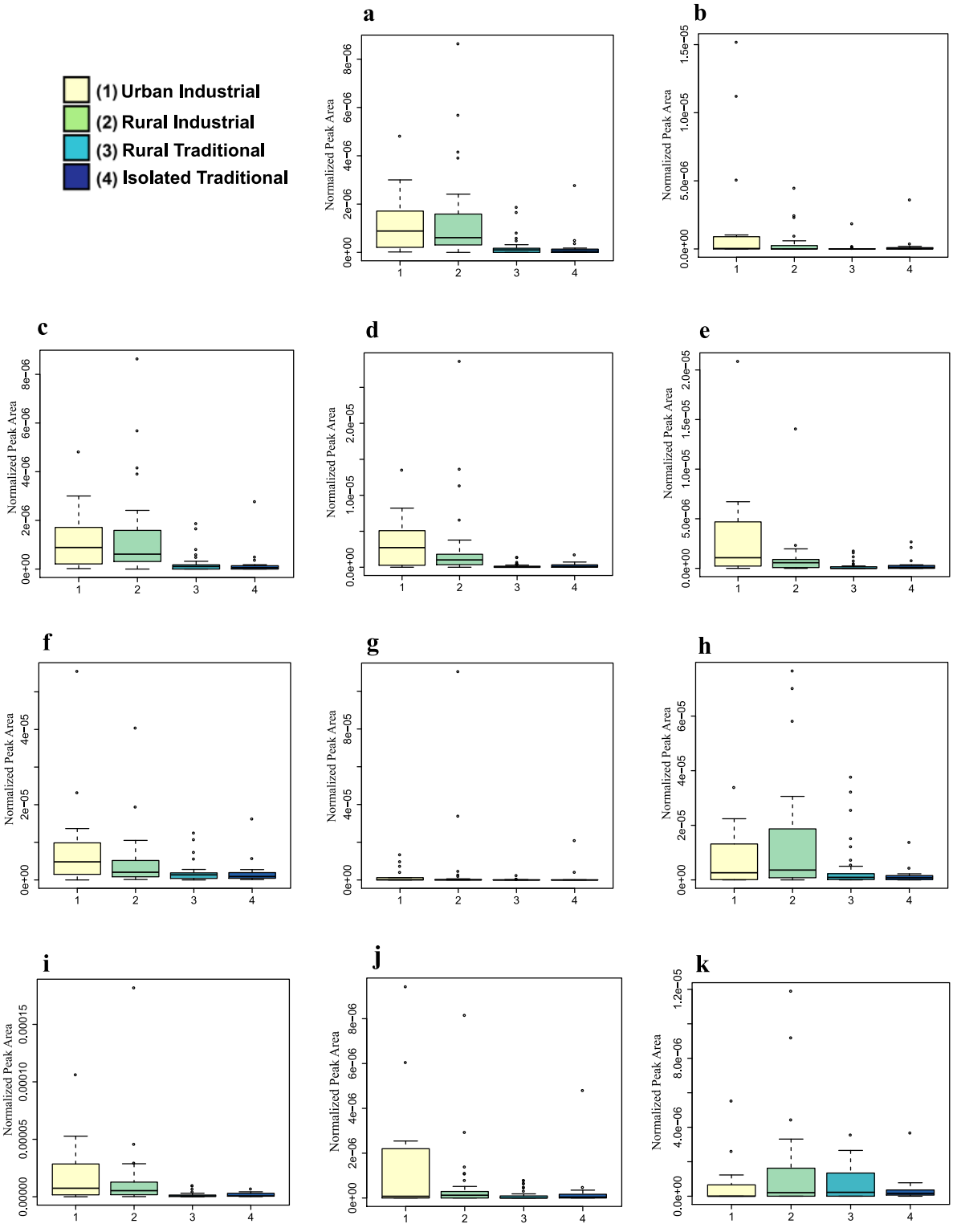

774

Supplementary Figure 2. Normalized abundances of amino acid-conjugated bile acids by industrialization score.

Same color key from **a** applies to figures **b**-**k. a,** leucocholic acid (Kruskal-Wallis p=1.69e-7); **b,** tyrosocholic acid (Kruskal-Wallis p=7.71e-3; **c,** glutamate-conjugated chenodeoxycholic acid (Kruskal-Wallis p=1.69e-7); **d,** tryptophan-conjugated chenodeoxycholic acid (Kruskal-Wallis p=4.9e-7); **e,** aspartate-conjugated chenodeoxycholic acid (Kruskal-Wallis p=1.13e-5); **f,** histidine-conjugated chenodeoxycholic acid (Kruskal-Wallis p=6.41e-3); **g,** histidine-conjugated cholic acid (Kruskal-Wallis p=0.04); **h,** leucine-conjugated chenodeoxycholic acid (Kruskal-Wallis p=0.04); **i,** tyrosine-conjugated deoxycholic acid (Kruskal-Wallis p=1.61e-5). **j**, aspartate-conjugated cholic acid (Kruskal-Wallis p=0.05); **k**, threonine-conjugated chenodeoxycholic acid (Kruskal-Wallis p=0.4

787

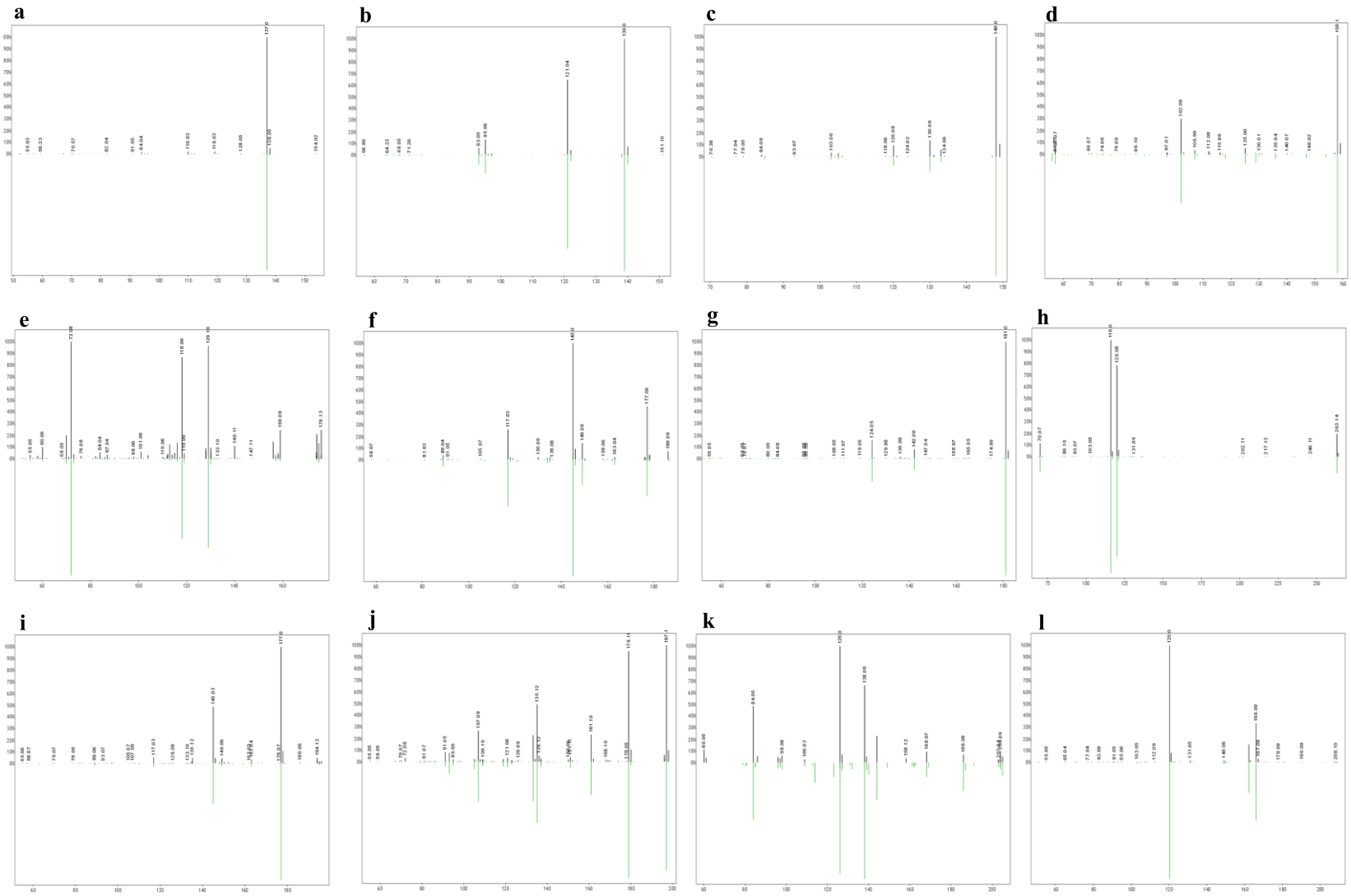

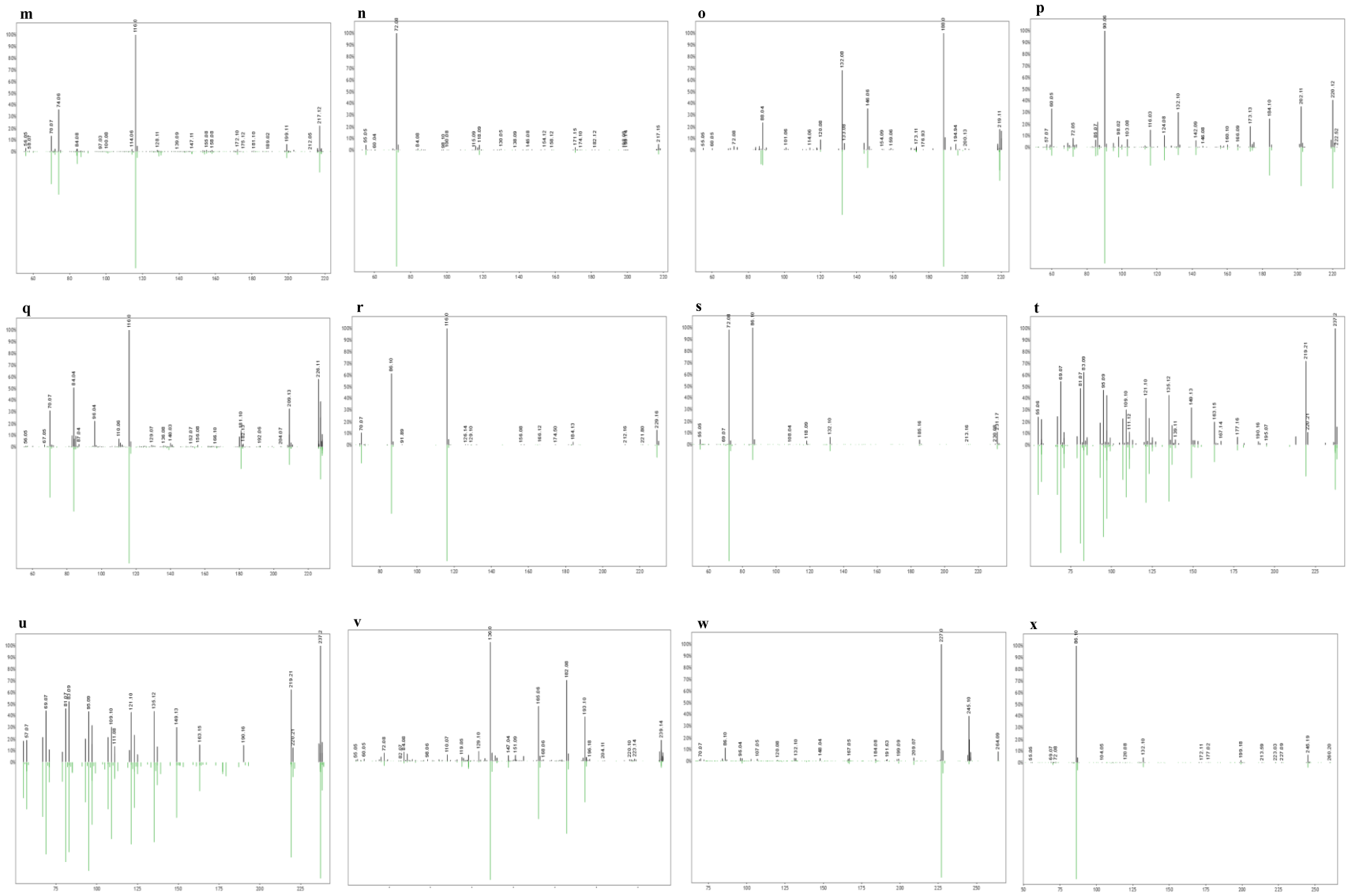

788

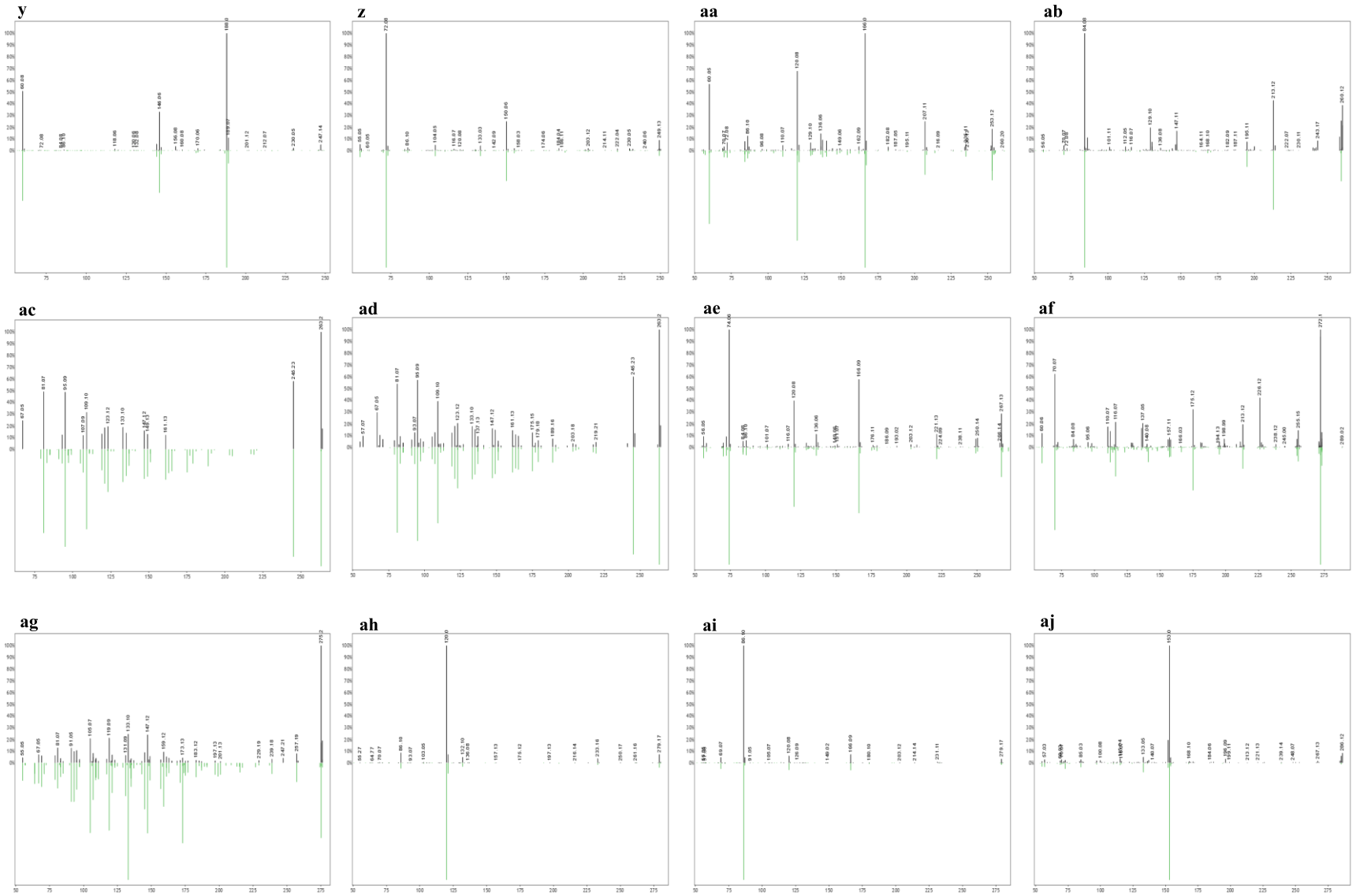

789

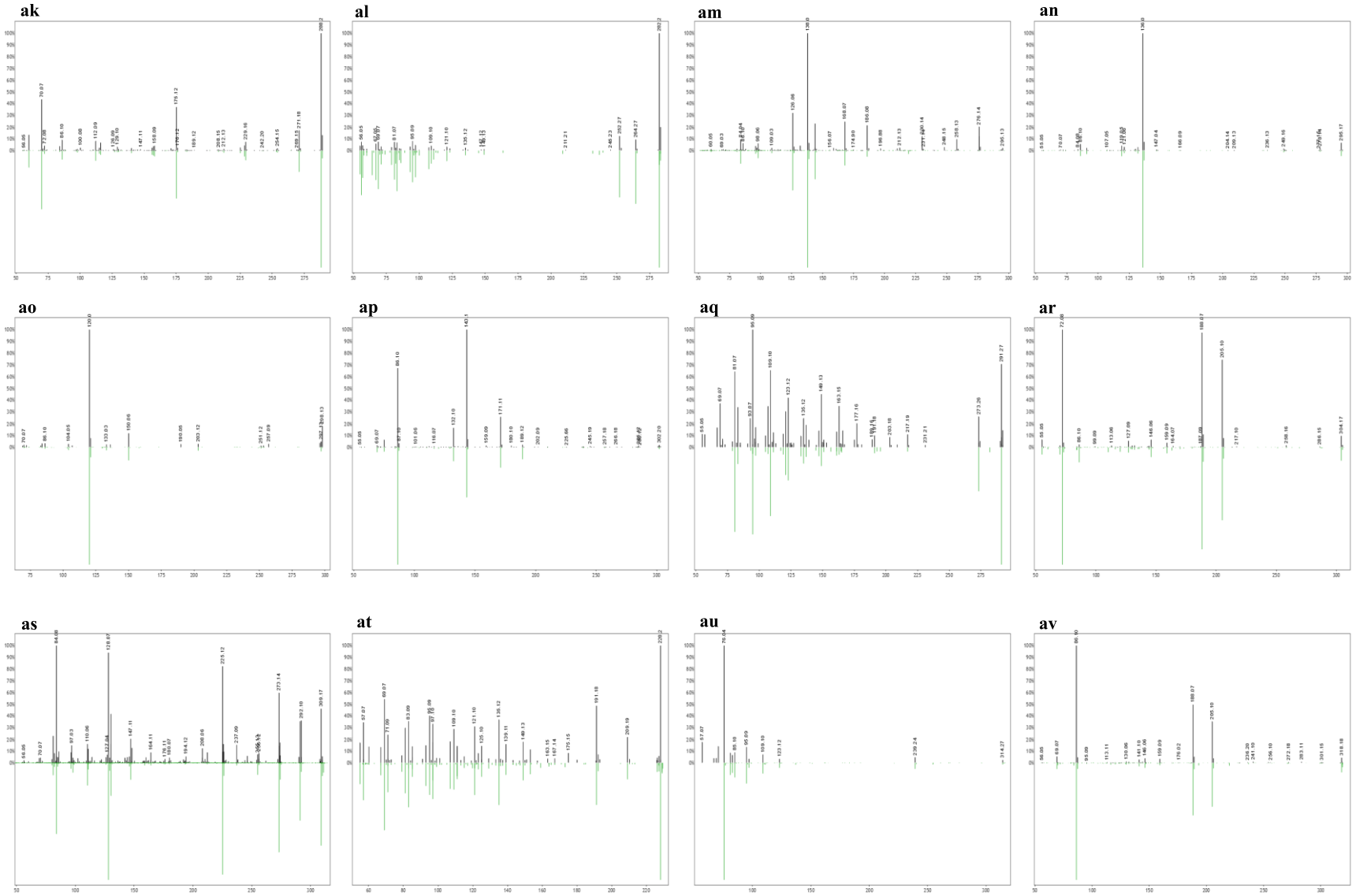

790

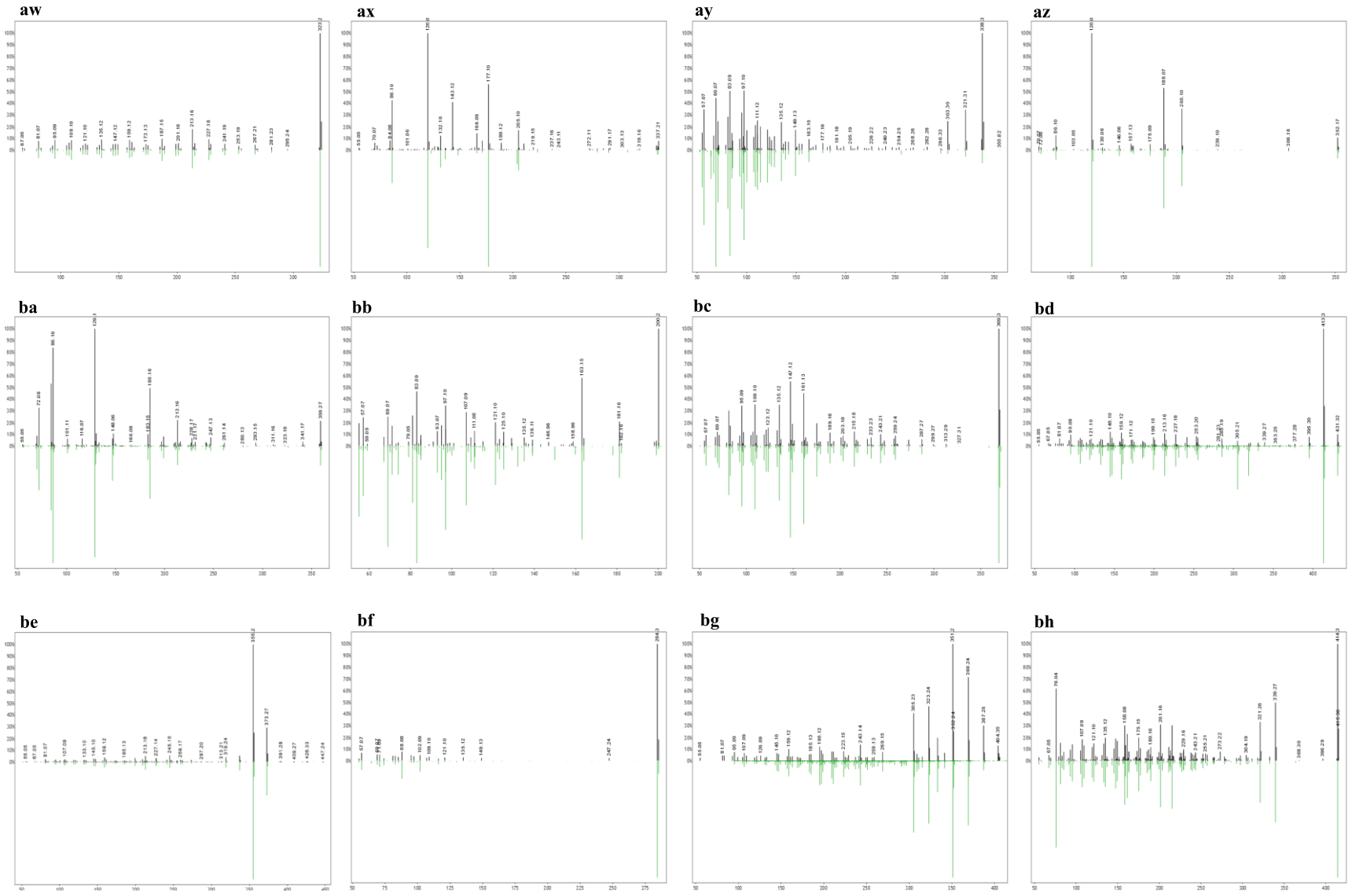

791

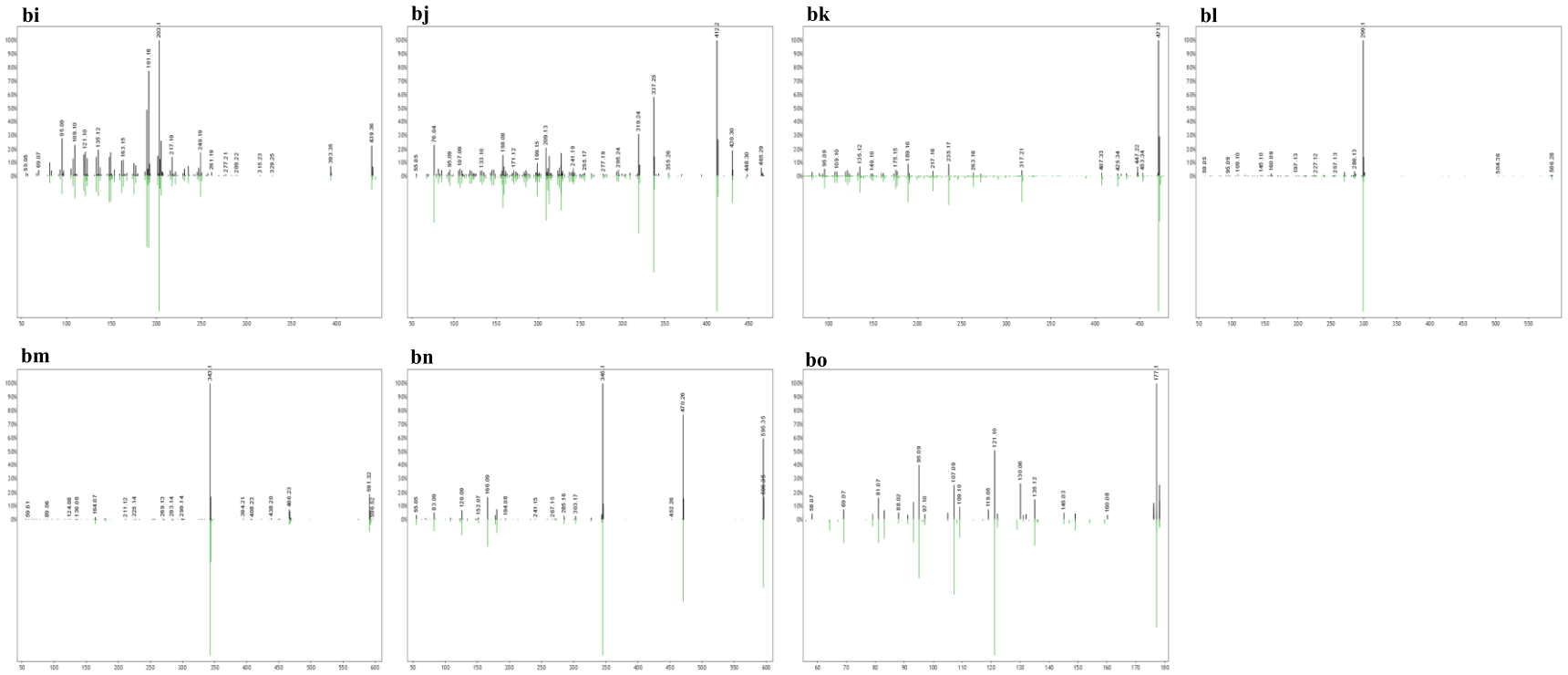

792 **Supplementary Figure 3. Mirror plots of core human fecal metabolites.**

Top black bars represent sample peaks for the respective metabolite, while bottom green bars represent library reference peaks. **a**, Hypoxanthine; **b**, Nicotinamide N-oxide; **c**, 3-methyl-2-oxindole (3-Methyloxindole); **d**, Hyocholic acid; **e**, Gly-Val (Glycylvaline); **f**, 3-Hydroxy-4-methoxycinnamic acid (Isoferulic acid); **g**, Paraxanthine; **h**, Phe-Pro (Phenylalanylproline); **i**, trans-Ferulic acid; **j**, Loliolide; **k**, N-Acetyl-D-mannosamine; **l**, N-acetyl-L-Phenylalanine; **m**, Thr-Pro (Threonylproline); **n**, Val-Val (Valylvaline); **o**, Abrine; **p**, Pantothenic acid; **q**, PyroGlu-Pro (Pyroglutamylproline); **r**, Ile-Pro (Isoleucylproline); **s**, Val-Ile (Valylisoleucine); **t**, cis-9-Hexadecenoic acid (Palmitoleic acid); **u**, Palmitelaidic acid; **v**, Gly-Tyr (Glycyltyrosine); **w**, Biotin; **x**, Leu-Leu (Leucylleucine); **y**, Lenticin; **z**, Val-Met (Valylmethionine); **aa**, Ser-Phe (Serylphenylalanine); **ab**, L-Saccharopine; **ac**, Conjugated linoleic Acid (10E,12Z); **ad**, Conjugated linoleic acid (9E,11E); **ae**, Thr-Phe (Threonylphenylalanine); **af**, Pro-Arg (Prolylarginine); **ag**, 9-OxoOTrE; **ah**, Phe-Leu (Phenylalanylleucine); **ai**, Leu-Phe (Leucylphenylalanine); **aj**, Xanthosine; **ak**, Arg-Ile (Arginylisoleucine); **al**, N-Tetracosenoyl-4-sphingenine; **am**, N-Acetylmuramic Acid; **an**, Tyr-Leu (Tyrosylleucine); **ao**, Phe-Met (Phenylalanylmethionine); **ap**, Ile-Gly-Ile (Isoleucylglycylisoleucine); **aq**, cis-11,14-Eicosadienoic acid; **ar**, Val-Trp (Valyltryptophan); **as**, Fructoselysine; **at**, Myristoleic acid; **au**, N-Palmitoylglycine; **av**, Ile-Trp (Iseoleucyltryptophan); **aw**, Lithocholic acid; **ax**, Leucine enkephalin; **ay**, 13-Docosenamide, (Z)- (Erucamide); **az**, Phe-Trp (Phenylalanyltryptophan); **ba**, Ile-Val-Lys (Isoleucylvalyllysine); **bb**, 3-Hydroxydodecanoic acid; **bc**, Cholesrol; **bd**, 6R)-2-(hydroxymethyl)-6-((3R,5R,7R,8R,9S,10S,12S,13R,14S,17R)-3,7,12-trihydroxy-10,13-dimethylhexadecahydro-1H-cyclopenta[a]phenanthren-17-yl)heptanoic acid; **be**, Cholic acid; **bf**, Octadecanamide; **bg**, (R)-4-((3R,5S,8R,9S,10S,13R,14S,17R)-3-hydroxy-10,13-dimethyl-7,12-dioxohexadecahydro-1H-cyclopenta[a]phenanthren-17-yl)pentanoic acid; **bh**, Glycoursodeoxycholic acid; **bi**, Oleanolic acid; **bj**, Glycocholic acid; **bk**, Enoxolone; **bl**, Bilirubin; **bm**, Urobilin; **bn**, Stercobilin; **bo**, 2-Butanone, 4-(2,6,6-trimethyl-2-cyclohexen-1-yl)

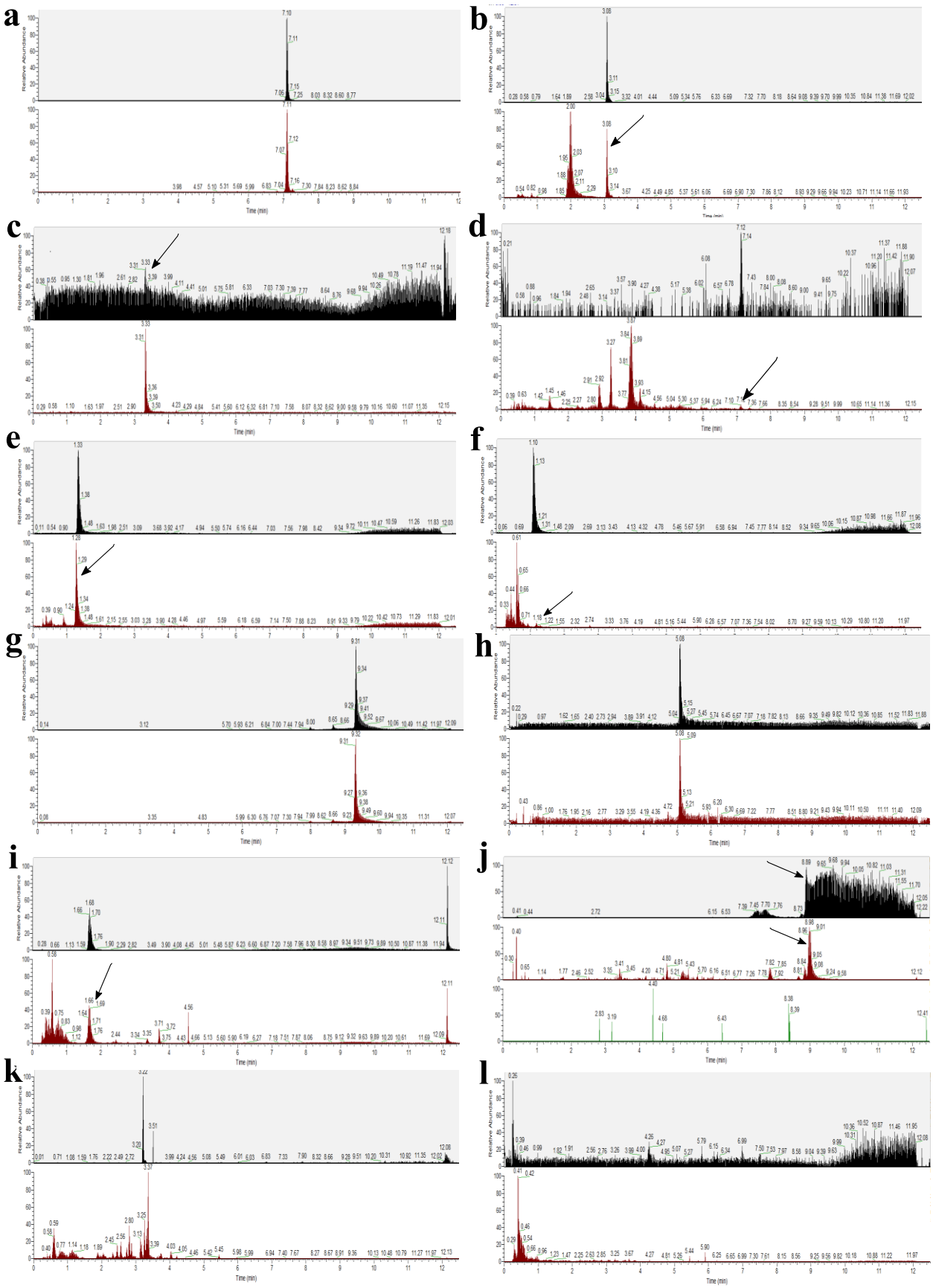

810

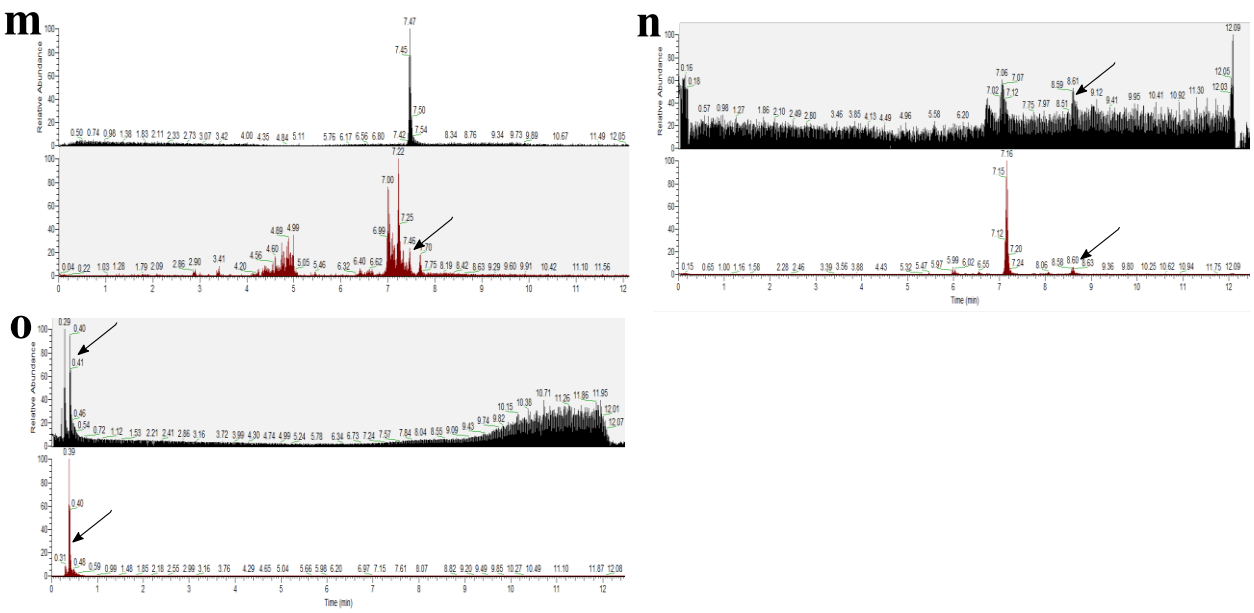

Supplementary Figure 4. Authentic standards validating sample annotations.
Standards are in black, representative samples are in red, blanks (if available) are in green. **a,** Enoxolone; **b,** N-acetyl-L-phenylalanine; **c,** trans-Ferulic acid; **d,** Lithocholic acid; **e,** Paraxanthine; **f,** L-Abrine; **g,** 13-Docosenamide, (Z)-; **h,** Hyocholic acid; **i,** Lenticin; **j,** Bilirubin. Included a blank (filtered to same *m/z*) to demonstrate standard has a distinct peak not seen in negative controls; **k,** Leucine enkephalin; **l,** L-Saccharopine; **m,** N-palmitoylglycine; **n,** Octadecanamide; **o,** Nicotinamide N-oxide.

822

823 **Supplementary Table 1. Metadata for individual samples.**

SampleID	Population	Industrialization Score	Sex	Age
NO01	Norman	1	M	23
NO02	Norman	1	F	37
NO03	Norman	1	M	40
NO04	Norman	1	M	26
NO05	Norman	1	M	28
NO06	Norman	1	M	28
NO07	Norman	1	F	32
NO08	Norman	1	F	32
NO09	Norman	1	F	34
NO10	Norman	1	M	41
NO11	Norman	1	M	26
NO12	Norman	1	F	27
NO13	Norman	1	M	35
NO19	Norman	1	F	32
NO20	Norman	1	M	26
NO21	Norman	1	M	23
NO22	Norman	1	M	26
NO23	Norman	1	F	26
GU1	Guayabo	2	F	52
GU2	Guayabo	2	F	19
GU4	Guayabo	2	F	40
GU6	Guayabo	2	NA	6
GU7	Guayabo	2	NA	9
GU10	Guayabo	2	F	58
GU11	Guayabo	2	NA	7
GU12	Guayabo	2	NA	16
GU13	Guayabo	2	F	41
GU16	Guayabo	2	NA	4
GU17	Guayabo	2	F	51
GU19	Guayabo	2	F	24
GU20	Guayabo	2	F	63
1TM	Tambo de Mora	2	F	61

2TM	Tambo de Mora	2	F	40
3TM	Tambo de Mora	2	NA	5
4TM	Tambo de Mora	2	F	40
6TM	Tambo de Mora	2	F	31
10TM	Tambo de Mora	2	NA	8
11TM	Tambo de Mora	2	M	39
14TM	Tambo de Mora	2	F	77
16TM	Tambo de Mora	2	F	38
17TM	Tambo de Mora	2	NA	7
18TM	Tambo de Mora	2	NA	13
23TM	Tambo de Mora	2	NA	1
24TM	Tambo de Mora	2	NA	1
26TM	Tambo de Mora	2	F	36
27TM	Tambo de Mora	2	NA	13
28TM	Tambo de Mora	2	NA	NA
31TM	Tambo de Mora	2	NA	28
TM10_01	Burkina Faso	3	M	55
TM13_01	Burkina Faso	3	M	53
TM23_02	Burkina Faso	3	F	51
TM01_01	Burkina Faso	3	M	55

TM09_02	Burkina Faso	3	F	32
TM11_04	Burkina Faso	3	F	40
TM17_02	Burkina Faso	3	F	35
TM20_03	Burkina Faso	3	F	37
TM22_03	Burkina Faso	3	M	29
TM25_03	Burkina Faso	3	F	38
TM29_01	Burkina Faso	3	M	73
HCO01	Tunapuco	3	F	36
HCO03	Tunapuco	3	M	6
HCO04	Tunapuco	3	M	4
HCO07	Tunapuco	3	F	3
HCO09	Tunapuco	3	NA	13
HCO10	Tunapuco	3	M	10
HCO11	Tunapuco	3	M	36
HCO12	Tunapuco	3	F	35
HCO13	Tunapuco	3	F	9
HCO14	Tunapuco	3	F	34
HCO15	Tunapuco	3	F	63
HCO16	Tunapuco	3	NA	11
HCO17	Tunapuco	3	F	7

HCO18	Tunapuco	3	M	11
HCO21	Tunapuco	3	M	10
HCO41	Tunapuco	3	NA	54
HCO53	Tunapuco	3	F	44
HCO61	Tunapuco	3	F	20
HCO62	Tunapuco	3	M	NA
HCO63	Tunapuco	3	F	6
HCO64	Tunapuco	3	F	NA
HCO65	Tunapuco	3	F	NA
HCO66	Tunapuco	3	M	11
HCO67	Tunapuco	3	F	26
HCO68	Tunapuco	3	M	7
HCO69	Tunapuco	3	NA	9
HCO70	Tunapuco	3	F	40
HCO72	Tunapuco	3	F	5
HCO73	Tunapuco	3	F	NA
HCO74	Tunapuco	3	F	36
SM01	Matses	4	M	30
SM02	Matses	4	F	25
SM03	Matses	4	M	10
SM05	Matses	4	M	1
SM10	Matses	4	F	6
SM11	Matses	4	F	4

SM23	Matses	4	M	7
SM25	Matses	4	F	2
SM28	Matses	4	F	52
SM29	Matses	4	F	50
SM30	Matses	4	M	4
SM33	Matses	4	F	5
SM34	Matses	4	M	4
SM37	Matses	4	M	12
SM39	Matses	4	F	40
SM41	Matses	4	M	6

824

Supplementary Table 2. The core human fecal metabolome.

All annotations had a mass difference of 0 to library reference. Bolded rows represent features detected in all ReDU datasets.

Compound Name	***m/z***	**RT (min)**	**Cosine Score**	**Detected in 6-sample filtering**	**Detected in half-sample filtering**	**Detected in all-sample filtering**	**Predicted ClassyFire[74] Class**	**Description derived from PubChem[88] and HMDB[65]**	**Present in Human Fecal Metabolome Database[65]**	**ReDU[39] Chemical Explorer Associations**
Hypoxanthine	137.046	0.39	0.98	Yes	Yes	No	-	Purine derivative associated with inosine and uric acid in humans	Yes	Found in bacterial cultures (*Clostridium orbiscindens* CC43_001K)
Nicotinamide N-oxide	139.05	0.31	1	Yes	No	No	-	Precursor to nicotinamide-adenine dinucleotide (NAD+) in animals	No (found in blood)	Associated with *Staphylococcus lugdunensis*. Found in human skin, saliva, and fecal samples
3-methyl-2-oxindole (3-Methyloxindole)	148.076	3.22	0.93	Yes	No	No	Indoles and derivatives (55.56%)	Endogenous product of 3-methylindole	No	Found in bacterial cultures (*Gardnerella vaginalis* and *Collinsella* sp. 4_8_47FAA)
Hyocholic acid	158.154	4.78	0.83	Yes	Yes	No	Steroids and steroid derivatives (100%)	Mammalian bile acid	Yes	Largely found in bacterial culture and humans

Gly-Val (Glycylvaline)	175.107	0.36	0.91	Yes	Yes	Yes	-	Glycine and valine dipeptide	Yes	Found in bacterial cultures, associated with *Staphylococcus aureus*. Also associated with inflammatory bowel disease.
3-Hydroxy-4-methoxycinnamic acid (Isoferulic acid)	**177.055**	**4.13**	**0.97**	**Yes**	**Yes**	**No**	**Cinnamic acids and derivatives (9.09%)**	**Endogenous human metabolite; Also potential biomarker for coffee, wheats, sunflowers, etc.**	**Yes**	**Predominantly found in plant, food (such as fruits), and beverage samples. Also found in human caecum and fecal samples.**
Paraxanthine	181.072	0.81	0.94	Yes	Yes	No	Imidazopyrimidines (21.74%)	Primary metabolite of caffeine; Found in animals and some bacteria	Yes	Not in Chemical Explorer

Phe-Pro (Phenylalanylproline)	263.139	2.57	0.99	Yes	Yes	Yes	-	Phenylalanine and Proline dipeptide	Yes	Predominantly found in bacterial cultures (*Bacteroides dore*i CL03T12C01, *Prevotella histicola, Parabacteroides goldsteinii* CC87F, etc.) and some fungal cultures
trans-Ferulic acid	195.065	3.01	0.91	Yes	Yes	No	Cinnamic acids and derivatives (9.09%)	Abundant in plant cell walls	Yes	Predominantly found in plant, food, and beverage samples. Also found in human fecal and caecum samples. Associated with Chagas disease.
Loliolide	197.117	3.11	0.94	Yes	Yes	No	Benzofurans (13.79%)	Plant metabolite	No	Found in environmental and plant samples (*Cucumis melo*)

N-Acetyl-D-mannosamine	204.087	3.27	0.91	Yes	No	No	-	Bacterial metabolite; Precursor to *N*-acetylmannosamine	Yes	Found in a fungal culture (species not specified)
N-acetyl-L-Phenylalanine	208.097	2.84	0.95	Yes	Yes	No	Carboxylic acids and derivatives (10.39%)	Metabolite of phenylalanine; Frequently found in urine of humans with phenylketonuria	Yes	Found in bacterial (*Fusobacterium ulcerans* 12-1B, *Sutterella wadsworthensis* HGA0223, etc.) and some fungal cultures
Thr-Pro (Threonylproline)	217.122	0.46	0.96	Yes	Yes	No	-	Threonine and proline dipeptide	No	Found in bacterial culture, fungal culture, and animal samples (e.g., mice, rats, humans, etc.). Found in human fecal samples. Associated with inflammatory bowel disease

										samples. Also associated with *Staphylococcus aureus*.
Val-Val (Valylvaline)	217.155	0.45	0.97	Yes	Yes	Yes	Carboxylic acids and derivatives (12.86%)	Valine and valine dipeptide	Yes	Found in fungal cultures and human fecal samples.
Abrine	219.113	0.61	0.88	Yes	Yes	No	-	Associated with *Escherichia coli* metabolism	No	Found in food, beverage, plant, animal, fungal culture, and bacterial culture samples. Also found in human digestive tract, fecal, heart, caecum, skin, and blood samples. Found

										equally in human rural and urban samples. Associated with many different bacterial species (e.g., *Parabacteroides goldsteinii* CC87F, *Prevotella nigrescens* CC14M, *Bifidobacterium longum*, etc.)
Pantothenic acid	**220.118**	**0.56**	**0.81**	**Yes**	**No**	**No**	**-**	**Also called Vitamin B5; essential metabolite for carbohydrate, protein, and fat synthesis**	**Yes**	**Found in animal (human, mouse, rat, etc.) and environmental samples.**
PyroGlu-Pro (Pyroglutamylproline)	227.103	0.44	0.86	Yes	Yes	Yes	-	No information provided	No	Predominantly found in bacterial cultures (*Prevotella nigrescens*, *Bacteroides stercoris* CC31F, etc.),

										plant, and human fecal samples
Ile-Pro (Isoleucylproline)	229.155	0.76	0.98	Yes	No	No	-	Isoleucine and Proline dipeptide	No (found in blood and sweat)	Predominantly found in bacterial (e.g., *Prevotella denticola*; *Bacteroides stercoris; Parabacteroides johnsonii*, etc.) and fungal cultures
Val-Ile (Valylisoleucine)	231.171	2.82	0.88	Yes	Yes	Yes	-	Valine and Isoleucine dipeptide	Yes	Found in fungal cultures
cis-9-Hexadecenoic acid (Palmitoleic acid)	**237.221**	**6.49**	**0.95**	**Yes**	**Yes**	**Yes**	**-**	**Unsaturated fatty acid**	**Yes**	**Predominantly found in soil samples**
Palmitelaidic acid	**237.221**	**7.35**	**0.98**	**Yes**	**No**	**No**	**-**	**Trans fatty acid**	**Yes**	**Found in human colon, upper digestive tract, liver, and fecal samples. Also found in soil samples.**

Gly-Tyr (Glycyltyrosine)	239.102	0.44	0.95	Yes	Yes	No	-	Glycine and tyrosine dipeptide	Yes	Found in bacterial cultures (e.g., *Parvimonas micra*, *Fusobacterium nucleatum*, etc.)
Biotin	245.098	2.39	0.87	Yes	No	No	Biotin and derivatives (16.67%)	Also called vitamin H; essential human metabolite	Yes	Found in environmental, animal, and bacterial culture (e.g., *Escherichia coli*, *Staphylococcus aureus*, etc.) samples. Also found in human nasal cavity, skin, and saliva samples.
Leu-Leu (Leucylleucine)	245.186	2.4	0.98	Yes	Yes	Yes	Carboxylic acids and derivatives (12.86%)	Leucine and leucine dipeptide	Yes	Predominantly found in bacterial cultures (*Bacteroides stercoris* CC31F, *Clostridium cadaveris* CC44_001G, etc.) and fungal cultures (not

										specified). Also found in human fecal samples.
Lenticin	247.145	1.22	0.97	Yes	No	No	-	Found in lentil extracts; Possible lentil biomarker	Yes	Found in food, animal, and bacterial culture samples (e.g., *Staphylococcus aureus*). Also found in human urine, milk, blood, and saliva samples.
Val-Met (Valylmethionine)	249.126	0.56	0.95	Yes	Yes	No	-	Valine and Methionine dipeptide	Yes	Not in Chemical Explorer
Ser-Phe (Serylphenylalanine)	253.118	0.79	0.93	Yes	Yes	Yes	-	Serine and phenylalanine dipeptide	Yes	Found in fungal cultures, bacterial cultures (*Bacteroides stercoris* CC31F, *Clostridium cadaveris* CC88A, etc.) and human fecal samples

L-Saccharopine	259.129	0.31	0.78	Yes	Yes	No	-	Involved in lysine degradation	Yes	Found in bacterial culture (*Staphylococcus aureus* JE3) and fungal cultures (not specified)
Conjugated linoleic Acid (10E,12Z)	**263.237**	**7.52**	**0.93**	**Yes**	**Yes**	**No**	**Prenol lipids (5.36%)**	**Variation of conjugated linoleic acid; Found in meat dairy products of ruminants; Dietary supplement**	**No**	**Found in human digestive tract, liver, colon, and feces. Also found in environmental and fungal samples.**
Conjugated linoleic acid (9E,11E)	263.237	6.68	0.92	Yes	Yes	Yes	Prenol lipids (5.36%)	Variation of conjugated linoleic acid; Found in meat dairy products of ruminants; Dietary supplement	No (found in blood)	Found in environmental samples and fungal cultures. Also found in human upper digestive tract, liver, and feces.
Thr-Phe (Threonylphenylalanine)	267.134	0.48	0.94	Yes	Yes	Yes	-	Threonine and Phenylalanine dipeptide	Yes	Found in fungal cultures

Pro-Arg (Prolylarginine)	272.171	0.32	0.72	Yes	No	No	-	Proline and arginine dipeptide	No	Found in a fungal culture (species not specified)
9-OxoOTrE	275.201	4.42	0.8	Yes	Yes	No	-	Long-chain fatty acid	No	Found in fungal cultures and plant samples (*Zea mays* L. and *Cucumis melo*)
Phe-Leu (Phenylalanylleucine)	279.171	2.59	0.99	Yes	Yes	Yes	Carboxylic acids and derivatives (12.86%)	Phenylalanine and leucine dipeptide	No	Found in human upper digestive tract, colon, and fecal samples. Also found in bacterial cultures (*Parabacteroides goldsteinii* CC87F, *Prevotella nigrescens* CC14M, etc.) and fungal cultures (not specified)

Leu-Phe (Leucylphenylalanine)	279.171	3.47	0.98	Yes	Yes	Yes	-	Leucine and phenylalanine dipeptide	Yes	Found in animal, fungal culture, and bacterial culture (e.g., *Bacteroides dorei*, *Staphylococcus aureus*, *Propionibacterium acidifaciens*, etc.) samples. Also found in human intestinal, vaginal, and fecal samples
Xanthosine	285.083	0.4	0.9	Yes	Yes	No	-	Purine nucleoside	Yes	Found in built environment, animal, and bacterial culture samples.
Arg-Ile (Arginylisoleucine)	288.203	0.36	0.96	Yes	Yes	No	-	Arginine and isoleucine dipeptide	Yes	Found in food and animal samples. Also found in human stomach, saliva, spleen, and

										fecal samples.
N-Tetracosenoyl-4-sphingenine	282.279	6.09	0.95	Yes	Yes	No	Fatty Acyls (11.54%)	Ceramide assocated with cell physiology and some human pathologies	Yes	Not in Chemical Explorer
N-Acetylmuramic Acid	294.119	0.38	0.84	Yes	Yes	Yes	Carboxylic acids and derivatives (4.08%)	Component of bacterial cell walls	Yes	Found in animal samples. In humans, found in caecum and fecal samples.
Tyr-Leu (Tyrosylleucine)	**295.165**	**2.71**	**0.97**	**Yes**	**Yes**	**Yes**	**Carboxylic acids and derivatives (31.25%)**	**Tyrosyl and leucine dipeptide**	**Yes**	**Found in fungal and bacterial cultures (*Prevotella nigrescens* CC14M). Also found in human feces**

Phe-Met (Phenylalanylmethionine)	297.126	2.18	0.93	Yes	Yes	No	-	Phenylalanine and methionine dipeptide	Yes	Found in bacterial cultures (*Bacteroides stercoris* CC31F, *Prevotella bivia*, etc.).
Ile-Gly-Ile (Isoleucylglycylisoleucine)	302.205	3.04	0.94	Yes	Yes	No	-	Isoleucine, glycine, and isoleucine tripeptide	No	Found in animal and bacterial culture samples (*Staphylococcus aureus*, *Bacteroides dorei*, *Bacteroides stercoris*, etc.). Also found in human samples collected from different body parts (duodenum, jejunum, urine, ileum, colon, saliva, stomach, fecal, etc.)

cis-11,14-Eicosadienoic acid	291.268	5.54	0.79	Yes	No	No	Prenol lipids (5.36%)	Omega-6 fatty acid found in human milk	Yes	Found in bacterial culture (*Propionibacterium acnes*) and plant samples
Val-Trp (Valyltryptophan)	304.167	3.02	0.97	Yes	Yes	No	-	Valine and tryptophan dipeptide	Yes	Found in fungal culture, food, and animal samples. Also found in human jejunum, stomach, duodenum, vagina, spleen, ileum, and fecal samples
Fructoselysine	309.164	0.31	0.85	Yes	No	No	Carboxylic acids and derivatives (4.08%)	Potential biomarker for milk and milk products	No (found in blood)	Found in animal samples. Small percentage also found in food samples. Found in human jejunum, kidney, ileum, fecal, and blood samples

Myristoleic acid	227.201	5.94	0.94	Yes	Yes	Yes	-	Long-chain fatty acid found in all eukaryotes; Potential biomarker for some dairy products and other food (anchovies, dates, sunflowers, chocolate, etc.)	Yes	Predominantly found in environmental samples, such as soil.
N-Palmitoylglycine	314.27	7.34	0.86	Yes	No	No	-	Human metabolite with fatty acid group	No	Found in environmental and animal samples.
Ile-Trp (Iseoleucyltryptophan)	318.167	2.27	0.97	Yes	Yes	Yes	-	Isoleucine and tryptophan dipeptide	Yes	Found in bacterial cultures (*Bacteroides stercoris* CC31F, *Selenomonas noxia*, etc.). Small percentage also in animal and fungal cultures. Also found in

										human intestinal samples
Lithocholic acid	**323.273**	**6.84**	**0.97**	**Yes**	**Yes**	**Yes**	**Prenol lipids (11.11%)**	**Secondary bile acid**	**Yes**	**Found in human feces.**
Leucine enkephalin	336.192	3.22	0.77	Yes	Yes	Yes	-	Enkephalin peptide; Produced in brain	No (found in blood)	Found in bacterial cultures (*Parabacteroides goldsteinii* CC87F, *Parabacteroides merdae*, etc.)
13-Docosenamide, (Z)-(Erucamide)	338.342	9.19	0.83	Yes	Yes	Yes	-	Fatty amide	No	Found in human colon, upper digestive tract, liver, and fecal samples. Also found in bacterial cultures (*Peptostreptococcus sp.* CC14N,

										Bifidobacterium longum subsp. longum 44B, etc.) and fungal cultures
Phe-Trp (Phenylalanyltryptophan)	352.166	3.28	0.96	Yes	Yes	No	-	Phenylalanine and tryptophan dipeptide	Yes	Found in fungal cultures (species not specified)
Ile-Val-Lys (Isoleucylvalyllysine)	359.266	0.6	0.91	Yes	Yes	Yes	-	Isoleucine, valine, and lysine tripeptide	No	Found in animal and bacterial culture samples. Also found in human jejunum, duodenum, ileum, caecum, colon, vaginal, and fecal samples

3-Hydroxydodecanoic acid	199.169	5.35	0.99	Yes	Yes	No	Lactones (20%)	Medium-chain fatty acid	Yes	Found in environmental samples, plant samples, and some human feces
Cholesterol	**369.352**	**10.5**	**0.97**	**Yes**	**Yes**	**Yes**	**-**	**Animal sterol from body tissues and plasma**	Yes	**Found in plant and environmental samples.**
6R)-2-(hydroxymethyl)-6-((3R,5R,7R,8R,9S,10S,12S,13R,14S,17R)-3,7,12-trihydroxy-10,13-dimethylhexadecahydro-1H-cyclopenta[a]phenanthren-17-yl)heptanoic acid	431.318	5.25	0.86	Yes	Yes	No	Steroids and steroid derivatives (6.12%)	NA	No	Found in human feces (<18 years old)
Cholic acid	**426.318**	**5.19**	**0.98**	**Yes**	**Yes**	**Yes**	**Steroids and steroid derivatives (8%)**	**Bile acid produced in liver**	**Yes**	**Found in human GI tract and feces. Associated with urban samples. Also found in bacterial cultures**

Octadecanamide	284.295	8.55	0.77	Yes	No	No	-	Metabolite derived from stearic acid, found in plant and animal fats	Yes	Found in environmental and plant samples
(R)-4-((3R,5S,8R,9S,10S,13R,14S,17R)-3-hydroxy-10,13-dimethyl-7,12-dioxohexadecahydro-1H-cyclopenta[a]phenanthren-17-yl)pentanoic acid	**405.264**	**4.81**	**0.92**	**Yes**	**Yes**	**No**	**Steroids and steroid derivatives (46.15%)**	**NA**	**No**	**Predominantly found in bacterial cultures (*Bacteroides caccae*, *Bacteroides ovatus*,*Clostridium orbiscindens*, etc.). Also found in mouse and human digestive tract and fecal samples.**
Glycoursodeoxycholic acid	**414.301**	**5.01**	**0.9**	**Yes**	**Yes**	**No**	**Steroids and steroid derivatives (36.71%)**	**Secondary bile acid**	**Yes**	**Found in animal samples (rats and humans). Also found in human blood plasma, blood serum, urine, skin,**

										and fecal samples.
Oleanolic acid	439.359	7.62	0.92	Yes	No	No	-	Plant metabolite	Yes	Found in fungal culture, food, plant, environment, and beverage samples. In humans, found in caecum and fecal samples.
Glycocholic acid	**446.32**	**4.69**	**0.96**	**Yes**	**Yes**	**No**	**Steroids and steroid derivatives (13.04%)**	**Secondary bile acid**	**Yes**	**Found in bacterial culture (e.g., *Enterococcus faecium*, *Prevotella oralis*, etc.) and food samples. In humans, found in urine, jejunum, digestive tract, and**

										fecal samples.
Enoxolone	**471.347**	**6.92**	**0.86**	**Yes**	**No**	**No**	**-**	**Derived from plant metabolite; Commonly used as artificial sweetener**	**No (found in blood)**	**Found in human feces (largely individuals <18 years) and fungal cultures**
Bilirubin	**585.271**	**7.55**	**0.95**	**Yes**	**Yes**	**No**	**-**	**Bile pigment produced during heme breakdown**	**Yes**	**Found in upper digestive tract and feces of humans.**
Urobilin	**591.318**	**4.07**	**0.96**	**Yes**	**Yes**	**Yes**	**-**	**Responsible for yellow coloring of urine**	**Yes**	**Found in urban human colon and fecal samples.**
Stercobilin	**595.349**	**4.05**	**0.94**	**Yes**	**Yes**	**No**	**Tetrapyrroles and derivatives (53.85%)**	**Responsible for brown coloring of feces**	**Not available**	**Found in human fecal samples.**

	2-Butanone, 4-(2,6,6-trimethyl-2-cyclohexen-1-yl)	**177.164**	**3.15**	**0.83**	**Yes**	**No**	**No**	**-**	**Also known as 3α,7α,12α-trihydroxycholestanoic acid (THCA); Intermediate bile acid associated with metabolic disorders**	**No**	**Predominantly found in plant samples (*Cucumis melo*), bacterial culture (Bacteroides dorei; *Propionibacterium acnes*), and fungal cultures.**

827

828 **Supplementary Table 3. Correlated metabolite abundances for industrialization score groups.**
829

Metabolite Node *m/z*	Metabolite Node RT	Metabolite Annotation	Summed Metabolite Abundance at Industrialization Score 1	Summed Metabolite Abundance at Industrialization Score 2	Summed Metabolite Abundance at Industrialization Score 3	Summed Metabolite Abundance at Industrialization Score 4
137.046	0.3805	Hypoxanthine	2.49E+10	5.61E+10	1.01E+11	43640000000
139.0503	0.3108	Nicotinamide N-oxide	9.71E+09	1.62E+10	2.26E+10	8532100000
148.0759	3.2191	3-methyl-2-oxindole	7.41E+08	2.14E+09	4.58E+09	1499345262
158.154	4.7767	Hyocholic acid	3.18E+08	6.46E+08	7.86E+08	398800000
177.0547	4.1326	3-Hydroxy-4-methoxycinnamic acid	8.01E+07	1.13E+08	4.33E+08	226904586.4
177.1638	5.9084	2-Butanone, 4-(2,6,6-trimethyl-2-cyclohexen-1-yl)-	4.17E+07	1.93E+07	2.78E+07	5170839.765
181.0721	0.807	Paraxanthine	1.09E+09	1.51E+08	3.68E+08	6218745.074
195.0651	3.0126	trans-Ferulic acid	3.59E+08	2.30E+08	1.40E+09	1096021152
197.1165	3.0981	Loliolide	1.76E+07	1.11E+08	3.75E+08	80086416.57
199.169	5.3476	3-Hydroxydodecanoic acid	8.72E+07	3.33E+07	3.68E+07	29025942.95
204.0868	3.5276	N-Acetyl-D-mannosamine	1.78E+08	6.88E+08	9.54E+08	960951142.4
208.097	2.8411	L-Phenylalanine, N-acetyl-	3.20E+08	1.40E+09	2.04E+09	950700000
217.1224	0.4618	Thr-Pro	3.33E+07	8.05E+07	1.42E+08	63401131.12
217.155	0.4485	Val-Val	8.18E+09	6.45E+09	2.96E+10	16681356835
220.1183	0.5571	Pantothenic acid	4.84E+09	8.72E+09	1.52E+10	5026000000

227.2005	5.943	Myristoleic acid	4.25E+07	3.65E+07	8.52E+07	62295962.54
229.155	0.7773	Ile-Pro	4.69E+10	5.93E+10	1.27E+11	65216000000
231.171	2.8229	Val-Ile	1.28E+09	1.96E+09	8.75E+09	5716297868
237.2214	6.4871	cis-9-Hexadecenoic acid	1.40E+08	7.36E+07	9.26E+07	203983532.6
239.1021	0.4404	Gly-Tyr	2.61E+08	5.24E+08	1.40E+09	1028935149
245.0983	2.3864	Biotin	6.21E+07	4.93E+07	1.84E+08	42932706.06
245.1862	2.3952	Leu-Leu	2.52E+09	3.45E+09	1.35E+10	9520700000
247.1448	1.2228	Lenticin	1.52E+08	8.26E+07	2.27E+08	25378613.53
249.1264	0.5559	Val-Met	1.07E+09	7.64E+08	2.35E+09	948787911.6
263.2369	6.6799	Conjugated linoleic acid (9E,11E)	3.87E+08	4.46E+08	1.19E+09	324224225.4
263.237	7.5172	Conjugated linoleic acid (10E,12Z)	1.54E+08	1.25E+08	4.39E+08	128896538.2
267.1342	0.4803	Thr-Phe	5.25E+08	6.05E+08	1.57E+09	482260542.5
272.1711	0.3211	Pro-Arg	2.32E+08	2.82E+08	6.76E+08	418814748.6
275.201	4.4249	9-OxoOTrE	3.78E+07	5.82E+07	9.97E+07	69862085.1
279.1708	3.4667	Leu-Phe	4.94E+08	5.45E+08	1.97E+09	1723342465
282.2791	6.0892	N-Tetracosenoyl-4-sphingenine	6.14E+07	5.07E+07	5.29E+07	20546244.6
285.0831	0.4016	Xanthosine	1.32E+08	3.20E+08	1.15E+09	274911286.4
288.2028	0.3645	Arg-Ile	5.46E+08	1.20E+09	5.44E+09	3715539067
291.268	5.5386	cis-11,14-Eicosadienoic acid	4.96E+07	3.97E+07	2.07E+07	805186.4409
294.1191	0.3764	N-Acetylmuramic acid	5.36E+08	4.07E+09	6.46E+09	1877551752
297.1261	3.1402	Phe-Met	9.42E+06	3.49E+07	7.51E+07	23615664.4
302.2048	3.0495	Ile-Gly-Ile	2.11E+07	2.41E+07	6.02E+07	12623338.92
304.1663	3.017	Val-Trp	9.20E+07	2.01E+08	5.42E+08	370977408.1
309.1635	0.3129	Fructoselysine	8.26E+07	1.01E+08	2.48E+08	229202252.1

318.1674	2.2699	Ile-Trp	4.22E+06	4.16E+06	2.50E+06	5691574.455
323.2734	6.8392	Lithocholic acid	7.89E+07	1.12E+08	6.91E+07	43717480.88
336.1923	3.2198	Leucine Enkephalin	8.38E+08	5.57E+08	9.79E+08	756900000
338.3419	9.1869	13-Docosenamide, (Z)-	1.21E+08	1.87E+08	3.05E+08	163546639
359.2661	0.5962	Ile-Val-Lys	6.59E+08	5.47E+08	1.27E+09	796505678
369.3517	10.5045	Cholesterol	9.83E+08	2.74E+08	4.91E+08	256617172
405.2639	4.8148	(R)-4-((3R,5S,8R,9S,10S,13R,14S,17R)-3-hydroxy-10,13-dimethyl-7,12-dioxohexadecahydro-1H-cyclopenta[a]phenanthren-17-yl)pentanoic acid	1.08E+08	2.56E+08	1.66E+08	1487753381
439.3585	7.6154	Oleanolic acid	4.07E+08	4.28E+08	1.89E+08	24997439.71
471.347	6.9183	Enoxolone	7.79E+08	1.08E+08	4.68E+07	9346458.261
585.2723	8.8966	Bilirubin	1.51E+08	8.39E+07	1.11E+07	2115169.671
591.3181	4.0748	Urobilin	7.68E+10	5.65E+09	1.70E+09	3131747944
595.3486	4.0491	Stercobilin	1.36E+11	1.23E+11	2.19E+11	47140614012
839.5646	5.1216	Cholic acid	6.37E+08	2.53E+09	4.27E+08	258646224.3

830

Supplementary Table 4. Public MassIVE datasets used for ReDU co-analysis.
NA values represent data labeled "not collected".

						Age Distribution (years)			Sex Distribution	
MassIVE Dataset Accession Number	MassIVE Title	MassIVE Project Description	MS Instrument	Sample Geographic Origin	Samples Used in ReDU Co-Analysis	0-17	18-44	45+	Female	Male
MSV000083559	GNPS - SEED Grant - Kim - very low birth weight infants	Very low birth weight infant fecal samples. Samples were extracted with ethanol and processed on a Thermo Q-exactive mass spectrometer coupled to C18 RP-UPLC for untargeted metabolomic analysis. Positive polarity acquisition of LC-MS/MS.	Q Exactive	United States	131	131	0	0	86	45

MSV000082433	GNPS_Amerindians_UrbanizationGradient	Human specimens (urine, feces, and skin) collected on swabs (wooden handle) from subjects living in Venezuela along an urbanization gradient (city to jungle). A collaborative project with Maria Gloria Dominguez-Bello.	Q Exactive	Venezuela	31	0	29	2	31	0
MSV000081351	GNPS - SEED Group - Eating behavior development in infants - Rhee	Data was acquired using a Thermo Q-Exactive and C18 RP-UHPLC.	Q Exactive	United States	309	188	112	0	207	101
MSV000083756	GNPS Extraction conditions benchmarking dataset	Generated by the Dorrestein lab, it consists of 4 samples extracted with different solvent or ratios of solvent.	Q Exactive	United States	63	0	0	63	0	63

MSV000083300	GNPS - Bacteriophage Subject 1	untargeted metabolomics. analysis of skin, feces, saliva, and nasal samples collected using swabs from a subject, subject 1, with bacterial infection treated using bacteriophage.	Q Exactive	United States	66	NA	NA	NA	0	66
MSV000081492	GNPS - SEED - Hyperbaric	Data was collecte on a LC-MS/MS system (c18 column) positive mode	Q Exactive	United States	21	0	10	7	9	8
MSV000082629	GNPS - ONR Primary Wright - Human-Stool	Data was collected on a LC-MS/MS system (c18 column) positive mode	Q Exactive	United States	75	0	75	0	30	45
MSV000082262	GNPS - SEED Grants - Sejal - Fecal	Data was acquired using a Bruker Maxis Impact and C18 RP-UHPLC using positive polarity of LC-MS/MS	impact	NA	113	108	1	0	51	60

MSV000082221	GNPS - SEED Grants - IBD Fecal	Data was acquired using a Bruker Maxis Impact and C18 RP-UHPLC using positive and negative polarity of LC-MS/MS	impact	United States	334	NA	NA	NA	166	167
MSV000082374	GNPS_Nobel_twin_study	Fecal samples from twins cohort (NOBEL study) to identify non-invasive biomarkers of disease severity in NAFLD	maXis	United States	143	0	53	90	92	46
Total	NA	NA	NA	NA	1286	427	280	162	672	601

848 **Supplementary Table 5. MZmine parameters for feature-based molecular networking.**

MZmine v 2.33

Method	Parameter	Value
Mass Detection	MS1	1.80E+05
	MS2	1.00E+03
Chromatogram Builder	Min time span (min)	0.01
	Min height	5.40E+05
	m/z tolerance (ppm)	1.00E+01
	Filter	MS1
Chromatogram Deconvolution - Local Minimum Search	Chromatographic Threshold	5%
	Search minimum in RT range	0.10 min
	Min relative height	15%
	Min absolute height	3.00E+05
	Min ratio of peak top/edge	2
	Peak duration range	0.01-1.5min
	m/z range for MS2 scan pairing	0.01
	RT range for MS2 scan pairing	0.1min
Isotopic Peaks Grouper	*m/z* tolerance (ppm)	1.00E-02
	Retention time tolerance (min)	0.05
	Max charge	3
	Representative isotope	Lowest *m/z*
	Monotonic shape	Yes
Join Aligner	*m/z* tolerance (ppm)	10
	Weight for *m/z*	5
	Weight for RT	1
	Retention time tolerance (min)	0.5
Peaks List Row Filter	Retention time (min)	0.2-12.51
	Min peaks per row	empty (leave unchecked)
	Keep only peaks with MS2 scan (GNPS)	yes
Gap Filling Peak Finder	Intensity tolerance (%)	75
	m/z tolerance (ppm)	1.00E+01
	m/z tolerance (*m/z*)	1.00E-06
	Retention time tolerance (min)	0.3
	RT correction	yes

Acknowledgements

We thank our collaborators with the Communidad Native Matses Anexo San Mateo, Caserío de Tunapuco, Centre MURAZ Research Institute, and the Ministry of Health in Burkina Faso for their collaboration and for opening their communities to our research. We thank Dr. Marielle Hoefnagels and students of the OU BioWriting class for their assistance with editing and reviewing the manuscript.

Author Contributions

C.M.L., L.-I.M., and K.S. conceived and designed the study. C.M.L., A.J.O.-T., R.Y.T., L.M.-R., E.G.-P., and L.T.-C. led Peruvian sample collection and developed ethical guidelines for community engagement. T.S.K. led fieldwork, metadata curation, and sample processing in Burkina Faso and contributed to lab work in the U.S. D.J. assisted with fieldwork in Burkina Faso, metadata curation, and conducted data analysis. L.-I.M. directed all LC-MS/MS experimentation and data analyses. J.J.H., E.H., and L.-I.M. acquired LC-MS/MS data. J.J.H. and L-I.M. performed LC-MS/MS data analysis with contributions from M.K., A.R.P., and K.F. J.J.H. wrote the manuscript with contributions from L.-I.M. and C.M.L. All authors reviewed the final manuscript.

Competing Interests

The authors declare no conflicts of interest.

Funding

871 This study was supported by grants from the National Institutes of Health (NIH R01
872 GM089886) and National Science Foundation (Doctoral Dissertation Improvement Grant
873 1925579).